2024-04-16

Multifunctional and Moisture Tolerant Zinc-Based Mono- and Bi-metallic Metal-Organic Framework (MOF) thin films

Emmanuel Agbata
Brigham Young University

Multifunctional and Moisture Tolerant Zinc-Based Mono- and Bi-Metallic

Metal-Organic Framework (MOF) Thin Films

Emmanuel Agbata

A thesis submitted to the faculty of
Brigham Young University
in partial fulfillment of the requirements for the degree of

Master of Science

Kara J. Stowers, Chair
Roger G. Harrison
Adam Woolley

Department of Chemistry and Biochemistry

Brigham Young University

ABSTRACT

Multifunctional and Moisture Tolerant Zinc-Based Mono- and Bi-Metallic
Metal-Organic Framework (MOF) Thin Films

Emmanuel Agbata
Department of Chemistry and Biochemistry, BYU
Master of Science

Many applications of metal-organic frameworks (MOFs) are highly dependent on their structures. The type and consistency of structure informs their properties. Zinc-based MOFs are applicable in different fields because of the low toxicity of zinc materials and are therefore also useful for catalysis. While MOF-5, a zinc-based MOF with carboxylate linkers is moisture intolerant, a variant of this has been found to be moisture tolerant. The introduction of a nitrogen-based linker in the zinc MOF which renders the structure moisture tolerant. This material has not been explored as much, despite its multifunctional properties. Furthermore, the growth of Zn-based bimetallics of this MOF has not yet been explored. In this work, we studied the synthesis of this zinc-based moisture tolerant MOF-5 as a thin film using a simple, fast, and cost-effective layer-by-layer wet synthesis method on different substrate surfaces. We successfully synthesized a series of bimetallics of this MOF as thin films on an untreated silicon wafer substrate. The successful synthesis of these materials was confirmed using X-ray photoelectron spectroscopy, X-ray diffraction and Raman spectroscopy techniques. Additionally, some software data analysis tools were used for characterization of the surface of the thin films to quantify the chemical composition. Future applications of these materials will be as sorbent materials for the capture of CO_2 and its subsequent conversion to CO which is a synthesis gas for different useful materials like fuel and other chemical materials.

ACKNOWLEDGEMENTS

TABLE OF CONTENTS

LIST OF TABLES

LIST OF FIGURES

CHAPTER 1: INTRODUCTION

1.1 Motivation of Work

Carbon dioxide is the greenhouse gas that poses the most concern for humans because daily domestic, industrial, and commercial activities increase the concentration of this gas in the atmosphere which in turn increases the risk of global warming. As a result of this, there is need to reduce the excess amount of CO_2 already present in the atmosphere and subsequently maintain carbon neutrality. According to the DOE, about 400 million and 1.8 billion metric tons of CO_2 needs to be removed from the atmosphere and captured from emissions sources annually by 2050. To remove carbon from the atmosphere, a different approach is needed, as the natural means of removing CO_2 from the atmosphere does not meet the increasing amount of CO_2 emitted, thus science and technology are employed. A different CO_2 removal approach involves the use of sorbent materials. Different materials have proven efficient in CO_2 removal. Some of them are porous polymers, metal-organic frameworks (MOFs), covalent-organic frameworks (COFs) and nitrogen containing compounds.[1] In this work, I aim to make a material that combines more than one property of these sorbent materials. The end goal is to support carbon neutrality which means that the amount of carbon emitted will be equal to the amount of carbon captured. CO_2, when captured can be converted into synthetic gas like carbon monoxide (CO) which is useful for making fuel and other useful chemicals and petrochemical products so we can recycle CO_2 (carbon neutrality). The end goal of this work is to engineer a cost-effective material that can efficiently serve a dual purpose of capturing and storing CO_2 and equally converting it to CO. For this work, I want to make a water stable zinc-based MOF that contains nitrogen groups which are effective binding sites for CO_2.[2]

1.2 Background of Metal-Organic Frameworks

Metal-organic frameworks (MOFs) attract a lot of attention because of their applications in areas such as electrochemical processes, catalysis, chemical sensing, optical and luminescence applications and as sorbent and storage materials.[3] As the name suggests, MOFs are made up of two parts: a metal center (node) and an organic ligand (linker) (Figure 1a).[4] These two components combine in an organized pattern to form a highly ordered crystalline material that has a high level of porosity and surface area. The surface area of a gram of a typical MOF is comparable to the area of a football field,[5] which is one of the main reasons MOF are good candidates for many applications such as interactions with gases and other sorbents. This material class is widely explored because it provides a high level of synthetic flexibility in both the ligand and metal centers. This flexibility makes it possible that MOFs can be manipulated to give a desired structure and property for specific applications.[6, 7]

MOF can be made of water intolerant and water stable structures depending on the interaction between the metal center and the ligand. The first framework denoted "MOF-5" is the MOF that contains a zinc metal center and benzene-1,4-dicarboxylic acid (BDC) *(Figure 1b)* with the general formula $Zn_4O(L)_3$ where "L" can be any possible ligand. The nodal points contain 4 tetrahedral zinc ions surrounded by a total of 13 oxygen atoms from the ligand molecules similar to the acetate secondary building unit (SBU) structure,[8] to form a well-ordered primitive cubic structure. The MOF-5 structure which has BDC as ligand is fairly water intolerant. A variation of moisture tolerant stable MOF-5 was discovered by substituting the BDC ligand with a carboxylic acid pyrazole ligand (3,5-dimethyl-4-carboxylic acid pyrazole) which is known as DMCAPZ *(Figure 1c)*.[6] The chemical property of the ligand allows this

version of the MOF to retain the cubic crystal structure of MOF-5. Additionally, the interactions between the Zn-node and the ligand provide an increase in water tolerance.

Figure 1a.
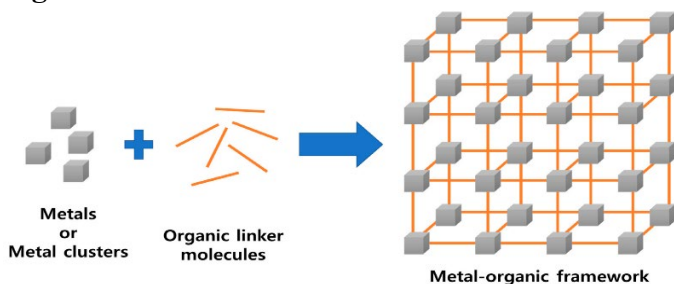
Figure 1b.
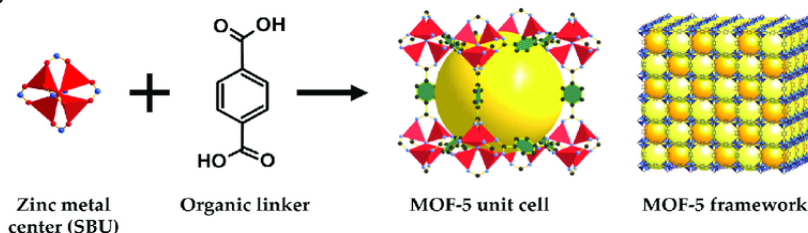
Figure 1c.
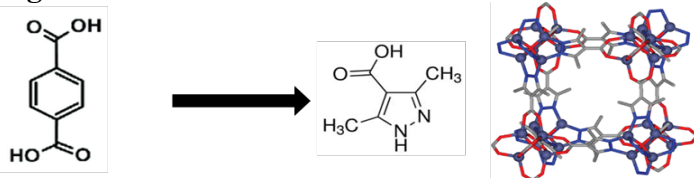
Figure 1: Theoretical image of MOF for (a) MOFs,[9] (b) MOF-5,[10] (c) Zn-DMCAPZ ligand difference[6]

Many different techniques have been used for the synthesis of MOFs including the sol-gel method, solvothermal method, electrochemical method, mechanochemical method, hydrothermal method, and microwave assisted method.[11-14] Most of these methods are used for the synthesis of powdered MOF crystals which are made in large quantities and take long times for the final product to be obtained (about 24 hours on average). The solvothermal method is the most used synthesis method as it does not require any specialized equipment and is the most

robust method for obtaining a high yield of MOF crystals. This method involves dissolving the metal and ligand precursors each in a solvent and then combining them and allowing them to react at elevated temperature and pressure as these are typically heated in an autoclave for specific period.[8] For example, the synthesis of Cu-BTC MOF powder was completed at 120°C for 3 hours, [15] while the synthesis of $[Cu_2(hfbba)_2(3\text{-mepy})_2]$ (Cu-F-MOF-4B) was carried out at 85°C for 96 hours.[16] While the synthesis of MOF crystallites can provide small nanoparticles in some cases, these nanoparticles are hard to deposit on wafers, and many of the applications for MOFs would be more amenable to the use of a thin film rather than powder. ***Table 1*** shows the methods for MOF synthesis and their compatibility with the synthesis of a MOF thin film.

Table 1: Synthesis methods of MOFs both as thin films and as bulk crystals.

Synthesis Methods	Powdered crystals	Thin films
Solvothermal Method	Yes	No
Hydrothermal	Yes	No
Microwave assisted	Yes	No
Electrochemical	Yes	Yes
Mechanochemical	Yes	No
Sono-chemical	Yes	No
ALD/CVD	No	Yes
Dip-coating	No	Yes
Spray coating	No	Yes
Spin coating	No	Yes
Pumping	No	Yes
Supersaturation crystallization	No	Yes

Synthesizing powdered MOF requires more time and energy. It also involves consumption of more precursor materials and produces more waste, so there is need to use a more economically beneficial synthesis approach, which led to the idea of making MOFs as thin films. Making MOFs into thin films has some advantages beyond the properties of MOFs. The thickness and morphology of a MOF thin film can be manipulated and tailored for applications in chemical sensing, catalysis, and photovoltaics. The fact that the thin films of MOFs are made at lower cost per synthesis of material with similar level of usefulness, compared to bulk crystal is an additional advantage. MOF thin films have improved surface area compared to the bulk crystal[17-19] due to higher surface to volume ratio.

There is some difficulty in growing MOFs as thin films. MOFs are made as thin films on substrate surfaces through the absorption of the nucleation points of the MOFs to the substrate surface-active sites. The nucleation points of the MOF are typically either the metal node or the organic linker which must interact with the surface-active sites such as an alcohol or a carboxylic acid. Silicon wafer is the most common substrate for the growth of thin films. The silicon wafer's active sites are silanol (-Si-OH) on the surface which act as the nucleation sites where a metal would typically bind to. If the metal sites are bound to the silanol groups, the ligands could then bind and cause MOFs to grow. Thin films of MOFs can be synthesized successfully through the layer by layer (LBL) method. LBL involves the deposition of layers of the film on the surface until the desired size and density and film thickness is achieved.[20, 21] The LBL approach applied to the synthesis of MOFs often involves the deposition of MOF thin films through the aid of precursor materials. Some deposition approaches include chemical vapor deposition, physical vapor deposition, atomic layer deposition and solution methods.[20, 22, 23]

The wet method of synthesizing MOF thin films has been widely explored as a type of layer-by-layer approach for making MOF thin films. This involves making solutions of the precursors, followed by the step-by-step deposition of these solutions onto the substrate surface as crystallites *(Figure 2)*. Figure 2 shows an example of this synthesis approach of Cu-HHTP MOF where Cu^{2+} is the metal center and HHTP is the ligand.[24] The wet method includes dip-coating, spin-coating, spray-coating and pumping method. In this work, I explored the use of the wet approach in the synthesis of thin films which provides a pathway for rapid, ambient synthesis, but must start with water tolerant features of the metal and ligand precursors.
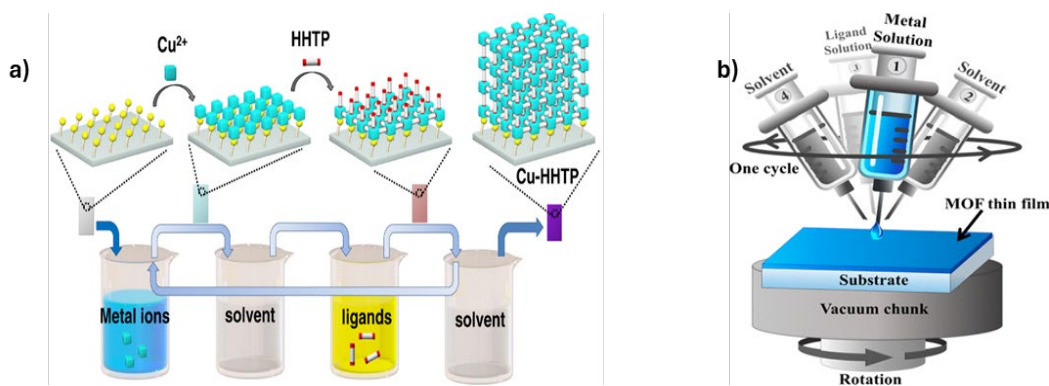
Figure 2: Different approaches for wet method of thin film growth (a) layer-by-layer,[24] (b)spin coating[25]

While the tunability of MOF is exciting, the ability to make thin films of MOFs is somewhat limited due to the challenges associated with the synthesis conditions. Although thin films of MOFs are important, due to the cheap cost and diverse applications, most MOFs are not stable to moisture and heat, so I wanted to make a MOF that would have high resistance to these conditions. Herein, the application of a simple, cheap, rapid, and reproducible spin coating method in the synthesis of MOF thin films is reported. In this work, I synthesized thin films of

zinc-based DMCAPZ MOF through this flexible and ambient condition optimized technique, by using a ligand that changes the chemical components of the MOF to afford a more water stable MOF compared to the BDC-MOF-5.[6]

Considering the high tunability of MOFs that involve changing both the ligand and metal center, many variations of MOFs are theoretically available for synthesis. Different methods have been applied for the synthesis of thin films of MOFs, but bimetallic thin films of MOF have not been widely explored despite its usefulness. The Zn-DMCAPZ MOF has not been explored. The reason why this is the case is because different metal centers have different sizes. But most importantly, depending on their coordination numbers, different metal nodes form different secondary building units,[26] thus, trying to combine different materials that like to form completely different secondary building units is hard, especially with thin film since these metals needs to nucleate by forming SBU on the substrate before the crystal growth starts to happen. The spin coating method was used at ambient conditions to synthesize the bimetallic thin film of DMCAPZ MOF-5. The synthesis of bimetallic-MOFs introduces an additional metal into the MOF framework and thus enhances and broadens the application of the MOF thin film, especially as applied to catalysis. These MOFs can be used for making bimetallic nanoparticle catalysts by removing the organic component of the MOF and revealing the nanoparticles through controlled agglomeration under tunable conditions. In this work, some of the commonly explored and more applicable metals were incorporated into the nodes (mental centers) during synthesis, to form bimetallic DMCAPZ MOF-5. In selecting these metals, the metals were selected based on the previous work involving electrochemical reduction of CO_2[27]. Also, they were selected because they are to zinc in the periodic table and have similar size and charge (Cu, Ni and Co). We also wanted to consider metals that are different from zinc both in terms of

charge and size (Al and Zr). These choices were made in order to explore how these differences and similarities affect the structure and properties of these materials. The quantitative and qualitative changes that are observed in the materials due to the incorporation of secondary metals were monitored and reported.

Many transition metals used in catalysis include an alloy or promoter to increase selectivity, conversion, or rates of the reaction. Due to the useful nature of multi-component materials in catalysis, bimetallic MOFs were explored to enhance and broaden the future applicability of this MOF. Some of the most used metals in catalysis are aluminum, nickel, cobalt, and copper. Nickel is useful for its role in hydrogenation reactions because it can be easily reduced and oxidized,[28] cobalt is popular for its use in desulfurization and oxidation reactions.[29, 30] Copper amongst other catalytic importance, is widely known for its use in CO_2 reduction, hydrogen formation and methanol conversion to formaldehyde.[31-34] Aluminum has also been widely studied for its use in copolymerization, CO_2 insertion and many fundamental organic transformation reactions.[34, 35] Zirconium aside from being a useful catalyst in green chemistry, is equally well known for its use in Michael addition reaction, oxidation reaction and its application in petrol petrochemical processes.[36, 37]

CHAPTER 2: METHODS AND CHARACTERIZATION

While thin films of MOF have been made and characterized through other methods, this chapter describes the use of a simple, low cost, and environmentally friendly approach for the synthesis of DMCAPZ MOF-5 thin films. This is a layer-by-layer method that applies liquid-phase-epitaxial growth to silicon wafers using spin-coating.

2.1 Growth of DMCAPZ MOF-5 thin films

2.1.1   Synthesis Materials and Reagents

a. Zinc-monometallic MOF thin film reagents

The metal node in the DMCAPZ MOF-5 is obtained from zinc salts such as zinc nitrate or zinc acetate; this is what is denoted as the metal precursor in the synthesis description. Zinc nitrate and zinc acetate have been widely explored as precursors for both bulk powder synthesis as well as other methods for thin film growth.[6, 38-42] Solutions of the metal precursor are made by dissolving a measured amount of the zinc salt in a solvent. N,N-dimethylformamide (DMF) was used as solvent due to the many reports indicating that large crystals are accessible and reproducible growth is documented.[38, 39, 41] Ethanol has reportedly been used and worked well as a solvent for synthesizing MOF-5.[6, 42] A dilute 5mM solution of the metal salt was prepared typically in volumes of 5-10 mL. 3,5-dimethycarboxylic acid pyrazole (H$_2$DMCAPZ) is used as the ligand precursor for the ligand solutions. A dilute 3mM solution of H$_2$DMCAPZ was prepared using the same solvent for the metal solution. The concentrations of the precursors were chosen to yield thin films with good crystallite quality, coverage, and less defects because concentration has to be high enough to support growth of thin film, but not too high that it leads to defects in the thin film crystals.[17, 42-44]

Both Zn-BDC and Zn-DMCAPZ have cubic crystal structure similar to a primitive unit cell (Figure 3). The structure of BDC MOF-5 is a cubic crystal structure where the zinc metal center forms a tetrahedral oxo-cluster with the oxygen from the ligands and thus the ligands are connected to the zinc center through the oxygen.[6] The DMCAPZ ligand differs from BDC in the following way: instead of binding to Zn through the two carboxylates of BDC, the binding is through one carboxylate, but the other side is like a zeolitic-imidazole framework (ZIF) motif since the pyrazole has similar binding to an imidazole in $H_2DMCAPZ$. Despite these differences, the coordination number, and the structure geometry of the two MOFs are similar. Therefore, macroscopically a cubic crystal of the thin film was expected, to give the first evidence that the right material has been synthesized.
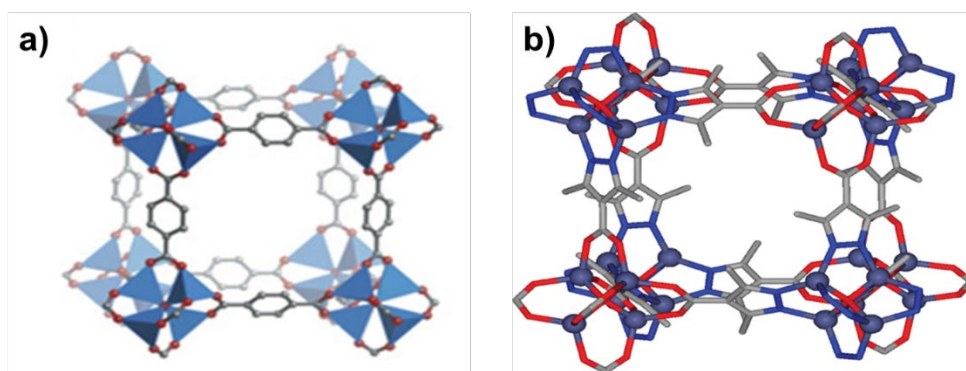
Figure 3: Side-to-side comparison of (a) MOF-5 (Zn-BDC),[10] and (b) Zn-DMCAPZ MOF [6]

b. Zinc-bimetallic MOF thin film reagents

To further improve the properties and applicability of this MOF, the Zn-DMCAPZ was doped with some of the common metals applied in catalysis as explained in Chapter 1 (see above). It is expected that a bimetallic MOF will have improved catalytic properties and its ability to be applied in the different catalyst aided reactions. The metals selected for this study

were chosen because those close to Zn in the periodic table have similar ionic sizes and properties which makes them more compatible with zinc. However, metals not near Zn were also incorporated to see how the effect differed based on size. DMCAPZ MOF-5 was doped with aluminum, cobalt, nickel, copper, and zirconium. The atomic radius of zinc is 0.133 nm which is smaller than those of Al and Zr that are 0.143 nm and 0.160 nm respectively. Zn on the other hand is slightly larger in size than Ni, Co, and Cu whose atomic radii are 0.125 nm, 0.125 nm, and 0.128 nm respectively. Zn, Co, Ni and Cu in MOF structures all have +2 oxidation state. Nitrate salts of Al, Ni, Co, and Cu have been reported for the synthesis of MOFs with high yield and good performance,[45-50] thus the nitrate salts of these metals were adopted for this synthesis process. In general, small amounts of the nitrate salts of the doped metals were used to make the metal precursor solution added to zinc acetate dihydrate to obtain bimetallic precursor solutions. The chloride salt of zirconium was used for making the solution used to synthesize the Zn/Zr-DMCAPZ MOF due to access considerations for the Zr metal precursor. Additionally, Ardila-Suárez *et al*. reported higher crystallinity for zirconium chloride compared to zirconyl chloride and zirconium nitrate for the synthesis of Zr-based MOFs.[51] For this work, zirconium chloride and zirconyl chloride were used for the bimetallic synthesis due to differences in growth for thin films compared to bulk solutions as discussed in the results Chapter 3 (see below). The solutions were made with 95% by mass zinc acetate dihydrate and 5% salt by mass of the secondary (dopant) metals. This ratio was chosen to facilitate the incorporation of these metals into the Zn MOF framework. At percentages higher than 5% (10% and above of the salt of the dopant metals), no growth of the MOF thin film was observed, so it was inferred that because of the differences in sizes and structures between these secondary metals and Zn, a lower percentage of

the dopant metals will promote successful incorporation of these metals into the zinc metal nodes.

c. Metal oxide substrates and properties

Silicon and aluminum-based substrates were explored because of their hydrophilic nature. This property supports the liquid phase epitaxial method by wetting the surface well, and therefore increases the likelihood of thin-film growth using a layer-by-layer approach. The solutions of the precursor materials were also prepared using hydrophilic solvents. Therefore, this property match between the substrate and the precursor solution hydrophilicity will enable favorable interaction between the substrate surface and the precursor ions in solution. In this study, polished silicon wafer, thermal oxide wafer (SiO_2) and sapphire (Al_2O_3) wafer surfaces were used. Each of these surfaces are commonly used in catalysis applications as inert supports in bead like structures. The interaction of the MOF thin films with each of these supports is important for understanding the diverse applications of the MOFs. It is important to understand what factors promote MOF thin film growth on each of these supports using spin coating method in order to readily interface these materials with different applications. Therefore, cataloging any factor(s) inherent in the substrates that can hinder the growth and thus the application of DMCAPZ MOF-5 thin film on the surface of these wafers is necessary.

The bulk chemistry of the silicon wafers are essentially made of Si-Si bonds in a tetrahedral form. However, at the surface, there is approximately 3nm layer of Si-O-Si bonding which terminates at the surface as Si-OH (silanol groups). The silanol group on the surface forms the point of attachment for the metals that nucleate and then grow MOF. The <111> orientation of the silicon wafer was used because it has been reported to ensure good success for the growth

12

of MOF thin films.[52, 53] In fact, according to Zhang, J.X. *et al*, the film grown on Si<111> had smaller sizes, lower strains, and less deformation.[53]

The wafer denoted as the thermal oxide silicon wafer is made by thermal oxidation of the Si-wafers to yield a thicker layer of silicon oxide (approximately 300 nm). This surface oxidation increases the number of nucleation sites, at the cost of no longer being conductive and therefore more difficult to image. The thermal oxidation process can be accomplished through a dry or wet process. Dry thermal oxidation is done in the absence of water vapor at a high temperature as shown below.

$$Si + O_2 \rightarrow SiO_2 \qquad\qquad \text{(eq. 1)}$$

This gives a denser layer of about 10-300 nm layer of silicon oxide. The wet thermal oxidation process takes place in the presence of water vapor to yield hydrogen gas and a thicker layer of silicon oxide.

$$Si + 2H_2O(g) \rightarrow SiO_2 + 2H_2 \qquad\qquad \text{(eq. 2)}$$

The SiO_2 layer after wet thermal oxidation is much thicker, typically about 0.12-2.4 μm. The thermal oxide used for this work is a <100> orientated wafer.

Sapphire is a thin cloudy transparent material made from pure Al_2O_3 crystal. The <0001> wafer was used for this work.

2.1.2   Thin film synthesis methods

There are several wet methods for the synthesis of MOF thin films including controlled growth through pumping continuous flow, dip-coating, spin coating, and spray

coating the substrate surface with the ligand and metal of the MOF *(Figure 4)*.[54] These are some of the wet methods used for the synthesis of MOFs.[7, 17, 42, 55] A bottom-up type of synthesis technique[56] involves the layer-by-layer deposition of the MOF thin film by exposing a substrate to a solution of the precursors in an alternating manner. The surface coverage and the size of the crystals depends on the number of cycles completed. More cycles give more coverage and larger crystallite size (if other synthesis conditions do not vary significantly).
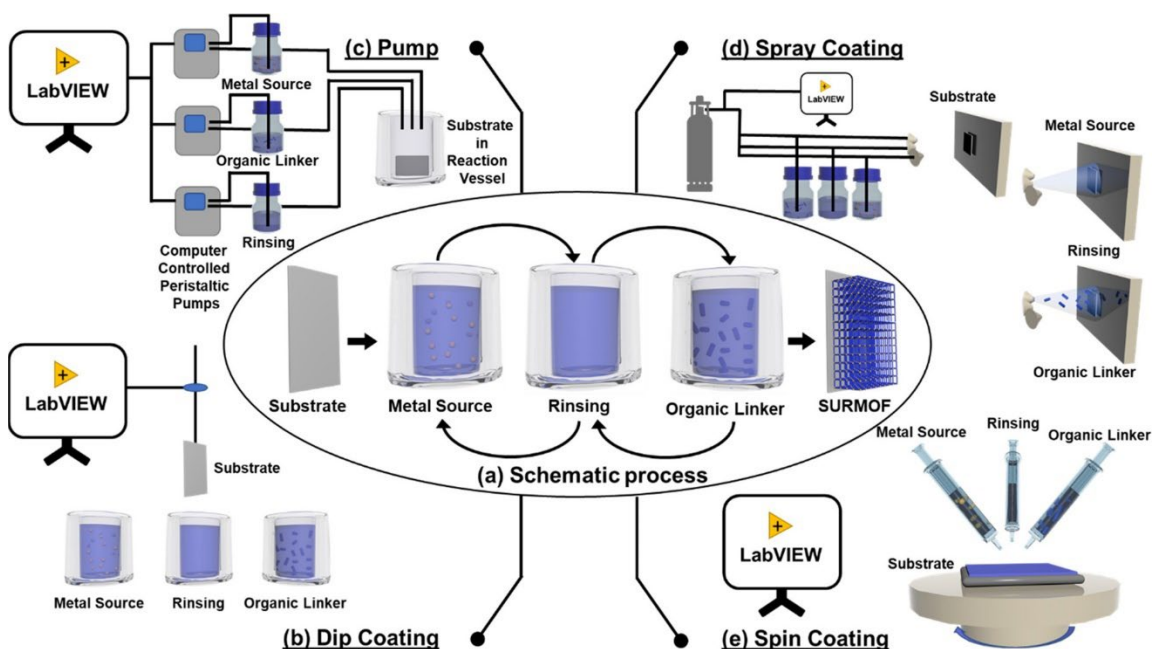
Figure 4: Approaches for layer-by-layer synthesis of thin films of MOFs [54]

In this work, the spin coating method was used for the synthesis of the MOF thin films as adopted from the work of Anderson, H. *et al.*[57] The variables associated with spin coating are temperature, relative humidity, solvent, precursors, and concentrations. When these variables are changed, the quantity (crystal size and density) and quality of thin film synthesized (crystallinity and defects) can be affected. The rotating rate or spin of the instrument (RPM) is chosen based

on the substrate wettability and the desired crystallite size whereas a higher spin rate yields lowers crystallite size. The volume of the solution and wash solvent are selected based on the wettability of the substrate and the evaporation rate of the solvent. The spinning process helps to spin off excess solution and solvent from the wafer surface and facilitates both nucleation of the films on the wafer surface. The metal precursor solution is introduced on the surface of spinning wafer through the aid of a micropipette, and after drying, the surface is washed by dropping 5μL the solvent used to make precursor solutions. Afterwards, the ligand precursor solution is introduced on the wafer and allowed to spin and dry off the substrate surface. Then, the wafer surface is again washed with the solvent used to wash the metal precursor solution to make a complete cycle. The last solvent is allowed to completely dry off the surface of the wafer and then the spinning was stopped by turning off the spin coater.

a. The spin coating process

5mM solutions of the metal precursor were prepared using DMF as solvent (99%, HPLC grade, Macron fine chemicals) and 3 mM solution of the ligand precursor was also prepared using the same solvent. The <111> oriented silicon wafer was cut into 2x2 cm samples. These samples were washed with ethanol and dried with lab air. The spin coater *(Figure 5)* is then turned on. The cleaned wafer is placed on the vacuum chunk of the spin coater. Vacuum was introduced that holds the sample firmly on the vacuum chuck of the spin coater. The spin coater was set to rotate at 2000 RPM. Small 5μL volumes were used for metal, ligand, and wash solutions. This process was repeated for 20 cycles. After completing the required cycles, the vacuum is turned off and the wafer was removed from the stage with the aid of a tweezer and placed in an ambient air oven to dry and remove any solvent for 24 hours at 150˚C.

Figure 5: Spin-coating machine image

After drying, the sample with the thin film is stored in a vacuum desiccator until it is imaged. The surface morphology and topography are characterized by imaging of the thin film using SEM or AFM.

b. Effects of synthesis conditions on the growth and properties of thin films

I. Humidity

All the wet synthesis methods require a liquid contact time for the formation of crystals. During the course of this research, It was found that the composition and crystallinity of thin films change during different seasons. Utah winters are dry, such that relative humidity is typically less than 20%. This leads to thin films composed of a large amount of amorphous material. I expect that the increased dry atmosphere combined with the spin coated solution on the substrate surface leads to insufficient time for the precursor solutions to interact with the substrate surface or with one another for proper nucleation and crystallization.[58] This creates an amorphous material on the surface instead of crystallite because the solutions dry off quickly. This is possible because spin coating is done under ambient conditions in which the

environmental effects are not entirely controlled. Completion of these thin films in a glove box would increase the unlikelihood of the environmental and seasonal effects.

Therefore, it is important to study and understand how the crystallization of the thin films on the surface can be controlled. Consideration of how the relative humidity of the environment can affect the types of solvent that was used to make our precursor solution is important for ensuring excellent thin film growth. Having this in mind, a small amount of water (1-5%) would be added to the solvent when the relative humidity of the laboratory environment was low (<20% rel humidity). The amount of water that is added into the solvent during the solution preparation is dependent on how low the relative humidity is. The lower the relative humidity, the higher the amount of water doped into the solvent. Added water was between 2 and 5% when the relative humidity was between 15 and 18%.

II. Temperature Studies

Due to the challenge associated with the use of zinc acetate as metal precursor, I decided to understand how temperature affects the growth of the MOF thin film, thus a temperature study was carried out. Zinc acetate easily decomposes to zinc oxide.[58-61] In this study the precursor solutions are subjected to different temperatures during the spin coating process. After the preparation and sonication of the precursor solutions, they were immediately poured into 10 ml beakers and placed into a water bath to obtain the desired temperatures. The set-up was maintained until the spin-coating process of all cycles was complete. However, the wash solvent was not heated. The solutions were heated to temperatures of 25° C (room temperature), 30° C, 40° C and 50° C. This study was used to monitor the changes in quality of the thin films as a function of temperature.

2.2 Characterization Techniques

The materials that is made can be characterized by using different techniques to determine their chemical and physical properties which will help identify the material and determine the success of synthesis. This characterization can be in the form of imaging (microscopy), light scattering, and spectroscopy. The explored techniques in this work include x-ray photoelectron spectroscopy, x-ray diffraction (XRD), atomic force microscopy (AFM), Fourier transformed infrared spectroscopy (FTIR), scanning electron microscopy and energy-dispersive x-ray (EDX) spectroscopy. These characterization techniques can be classified into the broad categories of vacuum and non-vacuum techniques which are described in detail below.

2.2.1 Vacuum techniques

Many characterization techniques require vacuum conditions to work due to electron scattering and analysis. To ensure that characteristic particles (electrons in this case) that are emitted from the materials are detected successfully without bumping into other particles and molecules in their path, a vacuum system is required. With a vacuum system, these interfering particles are eliminated so that a result with high quantitative and qualitative precision is achieved. The vacuum level required for each of these techniques varies. The vacuum techniques critical for understanding thin film properties are X-ray photoelectron spectroscopy, scanning electron microscopy and energy dispersive x-ray spectroscopy.

a. X-ray Photoelectron Spectroscopy

One of the surface sensitive spectroscopic techniques that gives the elemental composition of samples is X-ray photoelectron spectroscopy as shown in Figure 6.[62] Besides composition, information about the chemical and electronic state of elements can be obtained. It

can be used to quantify the amount of a given element present in the material relative to other components.

This technique involves the bombarding of the material with X-ray photon energy (hυ) that knocks off characteristic photoelectrons from the surface of the material. Although the X-ray photons go deep into the material and eject electrons, those electrons that are deep inside the material do not make it to the surface. Only those electrons close to the surface get knocked off completely from the materials and are detected, making XPS a highly surface sensitive technique. These photoelectrons, when released, travel with a specific kinetic energy. Knowing the energy of the X-ray photon beam and the kinetic energy of the released photoelectrons, the binding energy can be determined using the photoelectronic equation as shown in equation 3:

$$\textbf{E (h}\boldsymbol{\upsilon}\textbf{) = BE + KE + }\boldsymbol{\phi}_\textbf{s} \hspace{4cm} \textbf{(eq. 3)}$$

Where E is the energy of the photon and BE is the binding energy of the photoelectron and KE is the kinetic energy that the photoelectrons travel with and ϕ_s is the instruments work function, which is negligible, compared to the other components of the equation.

The XPS spectrum depicts electron counts per second on the y-axis and binding energy on the x-axis. Each element has a characteristic binding energy which is used to identify different elemental components of the material. The chemical state and chemical environment cause a slight shift in the binding energy of the elements. By properly fitting the peaks to their binding energies, all components of a material can be identified and quantified using XPS software.

The XPS spectrum can be in the form of a survey scan spectrum or a narrow scan spectrum. The survey scan shows the peaks of all the elemental components in one spectrum

while the narrow scan concentrates on the individual peak(s) of each of the component elements and so the narrow scan gives a spectrum with high resolution.
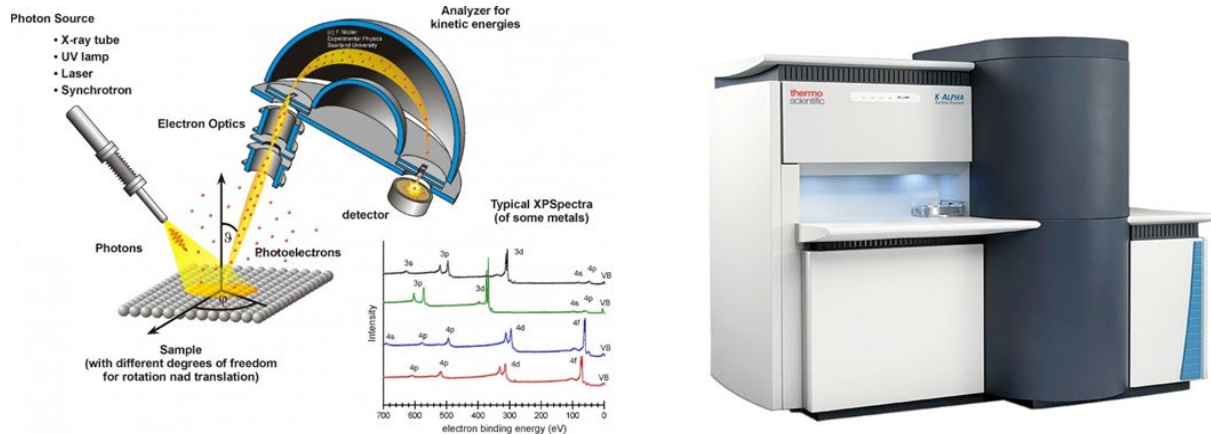
Figure 6: X-ray photoelectron spectrometer setup (courtesy: A.G Jacobs)

XPS was used to identify the elemental components and their chemical environments for the DMCAPZ MOF-5 thin films specifically for the nitrogen of the pyrazole part of the ligand and peak fitted using CasaXPS. This quantification allowed the determination of the different nitrogen species present in the sample. XPS was also used to determine the ratio of Zn and Si on the surface to determine the surface coverage of the films in the sample. The nitrogen components were also identified by studying the narrow scan of nitrogen which was useful in determining if there are different nitrogen species. Analysis and fitting of the peaks require creating background(s) and component peaks of each elemental present. The component peaks of the elements are determined by comparing the binding energy in the data to the binding energy in the database. Errors in fitting of the peaks were estimated and monitored using the standard deviation (SD) or the root mean square (RMS) values to ensure goodness of fits to obtain data that would yield reasonable conclusions.

b. Scanning Electron Microscopy

As shown in Figure 7, another vacuum technique is the use of an electron microscope for imaging the surface of materials. With the correct settings, materials can be imaged in the nanometer scale. This is thus useful in understanding the surface crystallite size of the MOF thin film material. In contrast to the optical microscope, the electron microscope uses electron beams as the source of illumination, and it therefore has higher resolution and can be used to observe smaller structures than can be visualized using an optical microscope.

This technique involves the release of high energy electrons using electron guns which are accelerated and then focused on the sample. The incident electrons on the sample can be absorbed, or backscattered and can even knock off sample electrons (secondary electrons) from the surface of the materials. X-rays are also emitted in this process. The most useful electrons for SEM imaging are the secondary electrons and the backscattered electrons. Both types of electrons need to make their way to the detectors and thus a high vacuum system is needed. The secondary electron images show the surface structure and morphology of the material. The backscattered electrons are used to identify the difference in average atomic mass of material based on image contrast. Those with higher mass produce more backscattered electrons and thus appear brighter.

When the number of electrons going into the material is less than the ones coming out, charges can be built up on the material. This effect is called charging and to reduce this effect insulating materials are coated with metal particles, such as gold, to improve conductivity. Silicon wafer has good conductivity without any coating, so it does not charge as much in SEM, but the other wafers such as thermal oxide and sapphire are less conducting. Sapphire substrate is

21

essentially non-conducting, so an SEM image of its surface cannot be clearly captured without a coating.
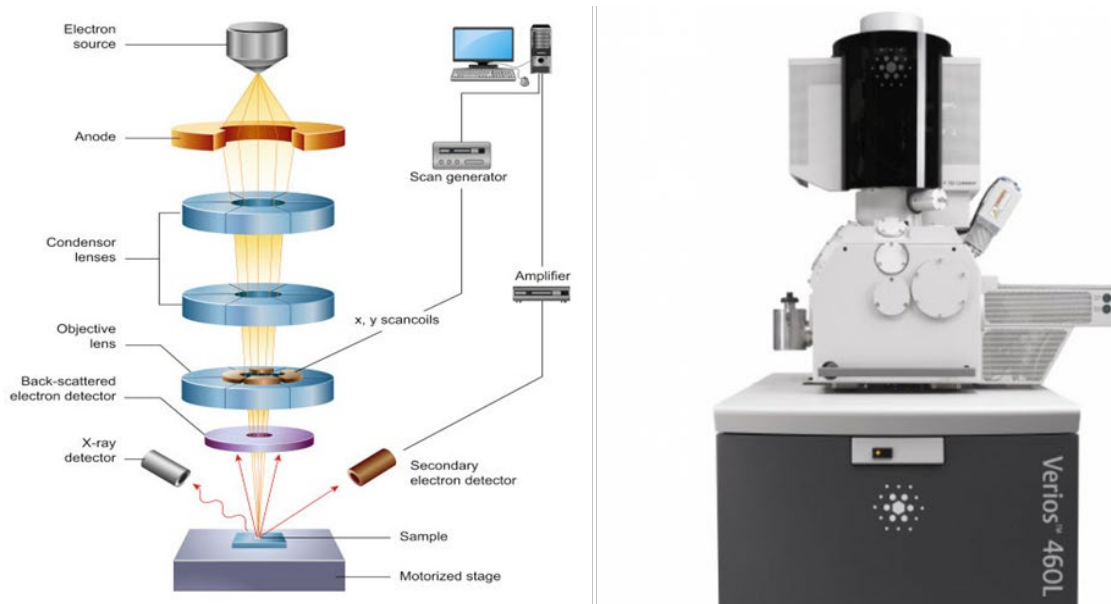
Figure 7: Scanning Electron Microscopy Schematic (courtesy: scimed)

ImageJ is a software image analysis tool that can be used for both quantitative and qualitative analysis and manipulation of microscopic and macroscopic level images. This program was used to estimate the crystal size and crystal density of the MOF thin films. The defects that exist in the structure and agglomeration of crystallites make the identification and quantification of the crystallite sizes and density challenging. The crystal sizes were therefore estimated using the edge-to-edge length of the crystal as shown in *Figure 8*. The crystal density was quantified by making small boxes in the image and the crystallites in each box were counted and the density number of crystallites per square area was averaged for all the squares and the mean was used as the crystallite density. About four boxes with an area of $300000nm^2$ were

counted and about an average of 83 crystals were counted per box. Due to the human errors associated with counting individual crystals and measuring their lengths, it was necessary to make provision for these errors using error bars. All the experiments were repeated at least twice and showed consistency before results were presented. Because the conditions vary from experiments to experiments, the crystal sizes and densities vary from one experiment to the other, but the general trends across samples are similar. This is why quantitative data is used for estimating and understanding the trends that exist across samples.
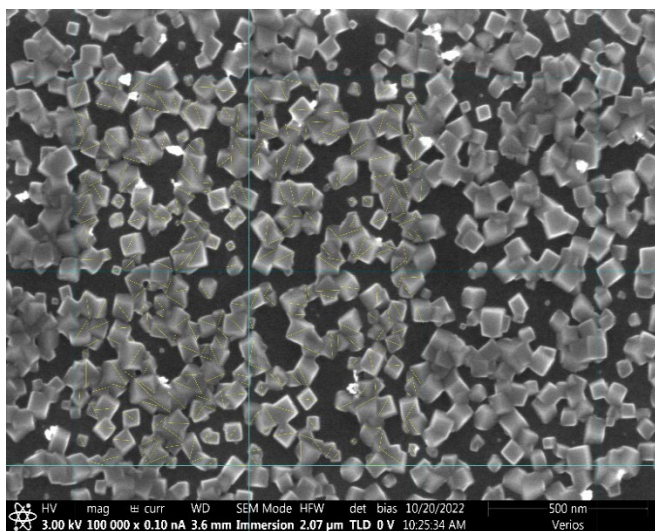
Figure 8: ImageJ analysis to determine surface density and crystal sizes.

c. Energy dispersive x-ray spectroscopy

This technique is used for elemental mapping of the material surface. It is a technique that is often coupled to the electron microscopic system. When the electrons are incident on the surface of the material, the ejected inner electrons leave vacancies in the atomic structures of the component elements and thus electrons occupying higher energy level drop in energy to fill these lower energy vacancies. The excess energy of these electrons is emitted as characteristic X-rays alongside the secondary electrons. The energies of these X-rays are characteristic of the elements they are emitted from (similar to the characteristic binding energies in XPS), and thus the

elemental components of the materials can be determined. Because the spot size is often small, SEM can be used with EDX for mapping. Another electron microscopic technique called transmission electron microscopy (TEM) is usually used to see the entire material since the electrons transmit through the material. This gives a more accurate crystal structure (shape) of the material. So, to determine the arrangement of elements within the entire material, TEM-EDX mapping technique must be employed.

EDX was used during imaging to determine amorphous and unwanted nanoparticle identity and composition. When a nanoparticle that was not the thin film of interest was observed on the surface on the SEM images, a portion of the material where the particles was found was then mapped using EDX to show the elements present within the mapped region based on the energy of the characteristic X-rays emitted from the sample surface. These characteristic X-rays are detected through the aid of the X-ray detector coupled to the SEM instrument. For this project, EDX was used in-situ, to determine elemental composition, but it was not used to study the surface of the materials because it is not very surface sensitive.

2.2.2   Non-vacuum techniques

There are other techniques that do not require a vacuum system to work. This is because they involve light beams that are either used for surface scanning, scattering, absorption, or transmission. The outcomes of these techniques generate information about molecular interaction, crystal structure and properties. The non-vacuum techniques that were used for characterization here include atomic force microscopy, X-ray diffraction, and infrared spectroscopy (IR).

a. Atomic force microscopy

AFM is an imaging technique *(Figure 9)*.[63] I adopted AFM for this work in order to image the insulating substrate samples with thin films on them because this technique does not have charging associated with it. Therefore, this technique was used with sapphire (Al_2O_3) and thermal oxide (SiO_2). AFM is one of the sub classes of scanning probe microscopy. It takes images of samples by scanning and probing the surface of the material.[54] It uses a cantilever which has a probing tip attached to it. The force between the probe and the sample surface depends on the stiffness of the spring (cantilever) and the distance between the probe and the sample surface. As the tip approaches the surface the attraction force between the tip and the sample causes the cantilever to bend towards the sample, but when it gets too close, a repulsive force exists, which pushes the cantilever away from the surface.
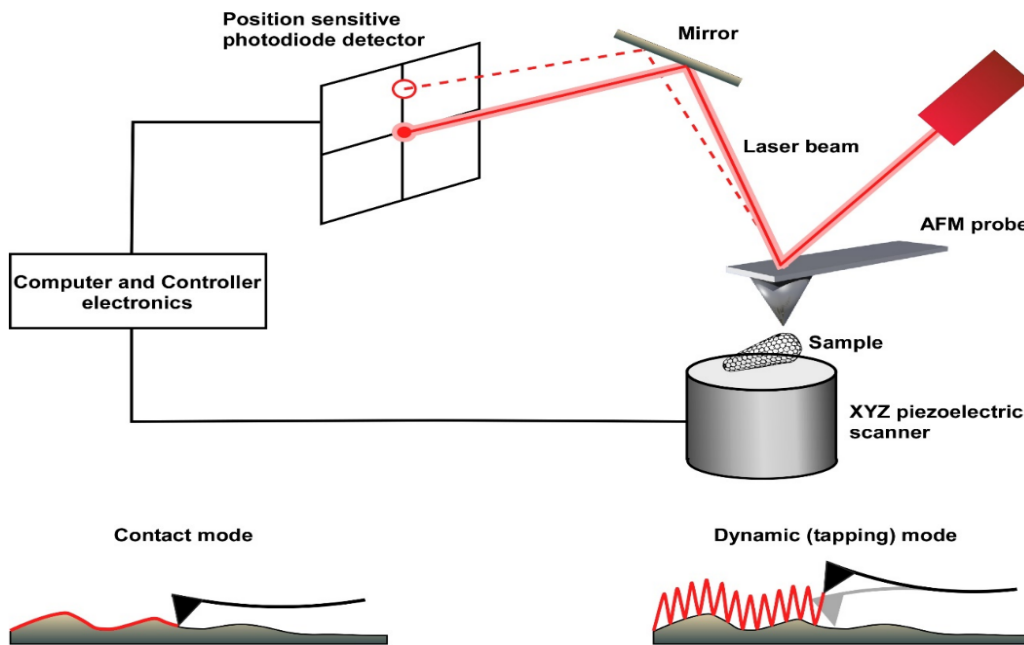
Figure 9: Schematic for imaging of material using atomic force microscopy[64]

In AFM, there is a z-scanner that is responsible for the up and down movement of the cantilever and an xy-scanner that moves the sample back and forth underneath the cantilever. A laser beam is positioned on the flat surface of the cantilever, and it reflects the position detector that records the bending of the cantilever. The beam is used to monitor the probing process and records the change in surface topography. This topographical mapping of the surface is converted to an image of the surface of the material. AFM imaging can be done using either the contact or the non-contact method. In the contact method, the tip is in contact with the sample surface but in the non-contact method, the tip does not contact the sample surface. It is just above the sample as scanning is done. The non-contact method preserves the sample from being damaged by the sharp tip and avoids wearing away of the tip which reduces image quality, thus non-contact saves operation cost. The instrument that was used is the Bruker nanoscope AFM and the scanasyst air mode (non-contact) was used for imaging.

The images for the substrate study were acquired using the AFM technique for good comparison between the different substrate surfaces and ImageJ was used to analyze the surface density and the crystallite sizes described above. The same error source and estimation techniques as SEM were also applicable to the AFM image.

b. X-ray diffraction

Another non-vacuum technique used to identify the crystal structure and properties of materials in X-ray diffraction. An X-ray beam is scattered/diffracted but at low enough energy to not eject the electrons (Figure 10). Different crystals of different materials have characteristic diffraction patterns that are unique to the atomic spacing within the unit cell. As the X-ray source shoots X-rays into the sample, the sample diffracts the X-ray, and the diffraction is picked up by

the detector. The angle at which the X-ray strikes the sample and is diffracted in a typical

powdered XRD system is called theta (ɵ). Peaks are formed if the X-ray from the top and bottom

path (separated by d spacing) reaches the detector at the same point. This is called constructive

interference, and the intensity of these peaks are plotted as function of 2ɵ. For the two rays to

reach the detector at the same time, *Ray 2* must travel through an additional path. Geometry is

used to derive an expression for this process as shown in equation 4.

$$\lambda = d\ (\sin\ ɵ) \tag{eq. 4}$$

The expression in *eq. 4* above represents the additional length travelled by the incident beam of

Ray 2. The refracted ray also travels additional length which is exactly equal to that of the

incident ray. Combining the additional path of the incident and refracted, equation 5 below was

obtained.

$$n\ \lambda = 2d\ (\sin\ ɵ) \tag{eq. 5}$$

These geometric relationships make up the components of Bragg's law which outlines the

conditions that must be met for constructive interference to happen to obtain a diffraction peak.
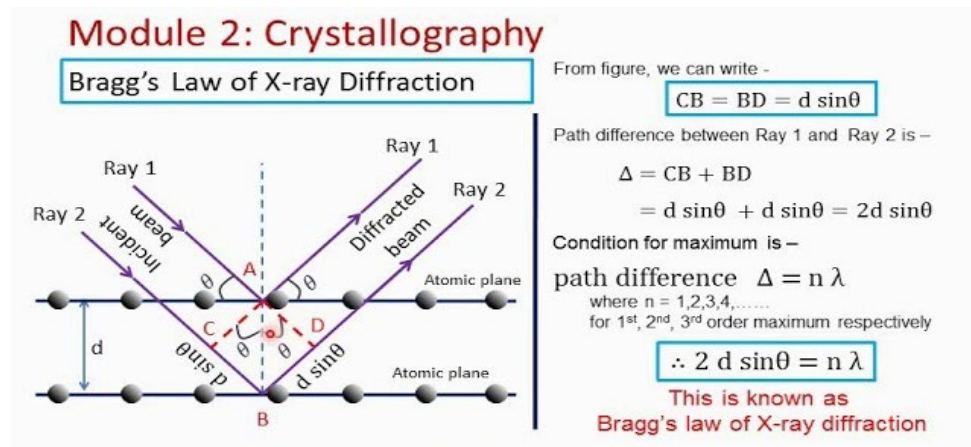
Figure 10: X-ray diffraction instrumental method (courtesy: Payaamvohra1)

Different materials and crystal structures have different diffraction patterns. This different diffraction pattern becomes a footprint that is used to identify different materials and the crystal structure(s) present in those materials when diffraction spectra are compared with the database and literature.

c. Infrared spectroscopy

A final technique used to study the thin film is through infrared radiation (IR). When IR is focused on a sample, the sample absorbs the radiation, and it causes vibration in the molecular bonds of the sample (Figure 11). This vibration can be symmetric stretching, anti-symmetric and deformation vibration.

When the light is passed through the sample through the infrared light source, most of it will pass through into the sample with only some of the light being reflected or transmitted. The light that is transmitted carries the molecular properties of the material and is collected at the detector. Fourier transformed IR spectroscopy uses an interferometer to detect the signal at different wavelengths simultaneously within a short time. The interferometer has a beam splitter that splits the beam into two; one goes to a fixed mirror while the other goes to a movable mirror and both are reflected to converge. These converged beams are then directed to the sample to give the molecular fingerprint of the sample in the form of intensity versus wavenumber.
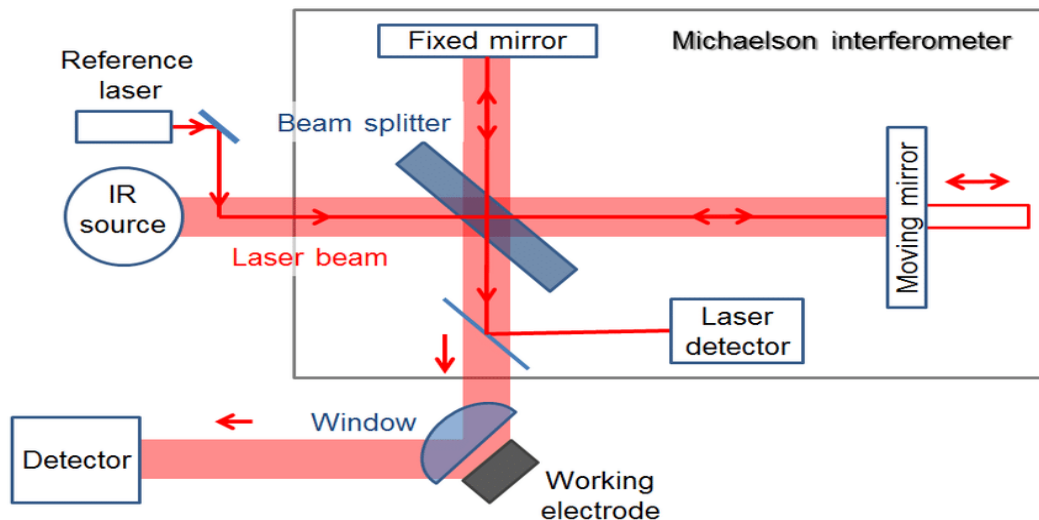
Figure 11: Schematic for Fourier-transformed infrared spectroscopy (courtesy: analchem resources)

In order to obtain these measurements, the sample was mounted on a magnetic film holder. The sample was mounted to expose the side of the wafer where the thin film is grown to be directly in line with the infrared beam source while avoiding interference from the composition of the tape used to mount the sample. The FT-IR was not used as a characterization technique because it requires ATR attachment, which we do not currently have.

d. Raman Spectroscopy

Raman spectroscopy is a technique that involves the detection of scattered light from a material (Figure 12). A specific energy of light is absorbed by the sample material. The resulting energy excites the electrons of this material into a virtual energy state (false or short-lived excited state). When the electron relaxes to the ground state (S_o), the light is emitted (scattered) with a specific wavelength. The scattering can be Stokes, anti-Stokes or Rayleigh depending on where the excited electron relaxes to, compared to where it was exited from. Stokes type of Raman shift happens when the electron relaxes to a higher energy level than where it started.

29

This leads to emission of energy and is viewed as a band with positive wavelength. The most common shift is the Stokes shift and that is what is used for the analysis of materials. When the electrons relax exactly into the same energy state as it was emitted from, Rayleigh scattering is said to happen and thus energy change is zero and this shows up as band at wavelength of zero. When the electron relaxes to a state of lower energy than it came from, energy is absorbed, and it shows up as a band with a negative wavelength. It is called anti-Stokes scattering shift. Anti-Stokes is not common.
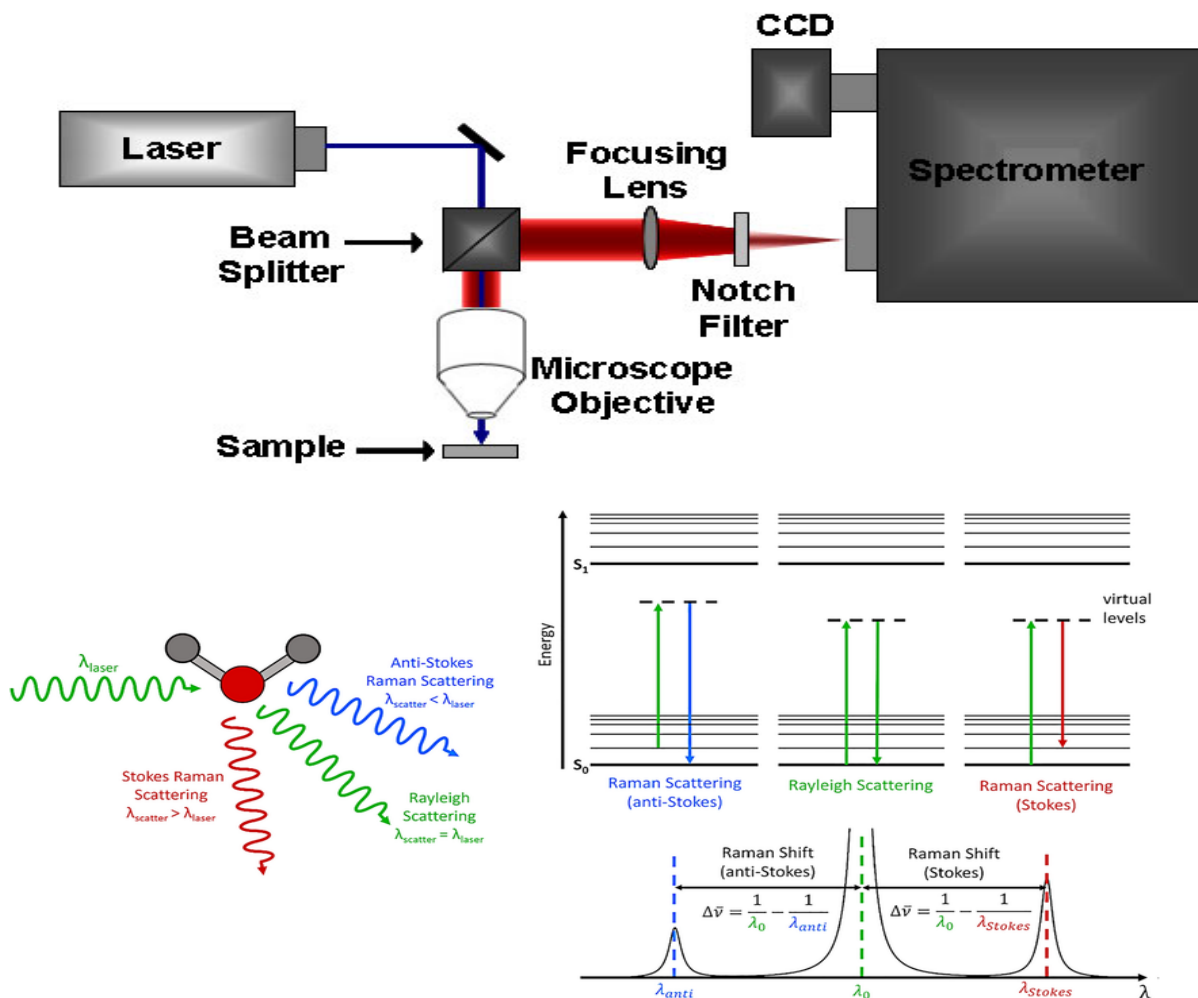
Figure 12: The schematic of the Raman instrument (courtesy: libretexts chemistry)

The Raman technique was not applied for these thin films because of the thinness of the films that is synthesized, which is not thick enough to be detected using Raman. The surface-enhanced Raman spectroscopy could work because it needs a special substrate that is coated with a highly conductive metal. This technique was not available for this work, so the Raman spectroscopic technique was not applied for the analysis of these samples.

CHAPTER 3: Results and Discussion

3.1 Initial growth and minimizing Zinc oxide nanoparticles

The synthesis of DMCAPZ MOF-5 Zn frameworks on SAM modified surfaces has been successfully reported using a pumping method.[55] No prior report of spin-coating a DMCAPZ MOF-5 thin film on a bare oxide surface is found in 2023 and 2024 when this project was initially started and completed. The synthesis of the Zn-based thin film with a MOF-5 structure using dimethyl carboxylic acid pyrazole (DMCAPZ) as ligand was achieved adapting a method as reported by Anderson *et al.*[57] The thin film was successfully obtained using zinc acetate dihydrate as a metal precursor in solution in a layer by layer spin-coating method, on silicon and thermal oxide wafers as oxide (***Figure 14)***. The similar cubic structures of the thin film appears in SEM and AFM images and is consistent with the structural arrangement of atoms.[6] The resulting thin film showed high crystallite density, considering that no preparation was done to increase surface silanol groups or nucleation sites beyond the inherent silanol groups that are present.

The growth of the moisture intolerant BDC MOF-5 was tried using the wet synthesis method used in this work, but the MOF-5 showed no growth at the first try ***(Figure 13a)*** try and a poor growth with amorphous looking materials on the background ***(Figure 13b)*** which shows that the crystallization of the thin films of Zn-BDC MOF is not favorable under a wet condition. The image in ***Figure 13b*** shows large cubic crystals with poor crystal density and a lot of particles on the sample surface.
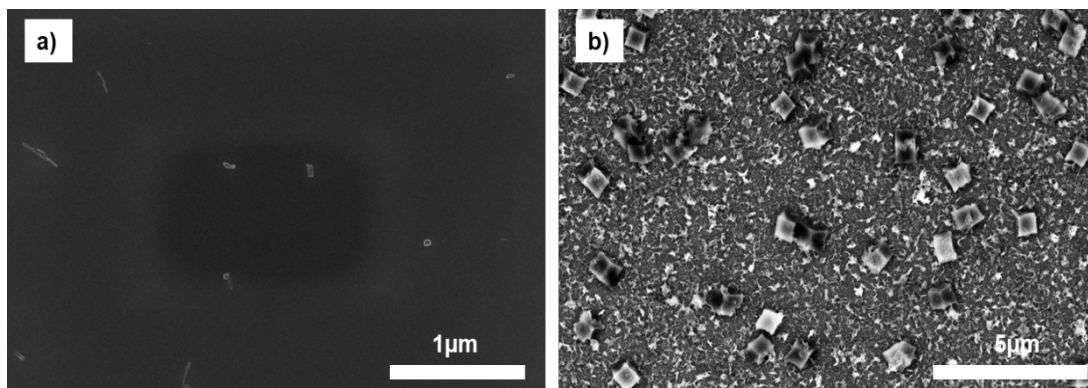
Figure 13: SEM image of moisture intolerant Zn-BDC MOF for (a) first try, and (b) second try on silicon wafer.

Unfortunately, initial conditions resulted in both MOF crystallites and ZnO nanoparticles as well as some amorphous material on the substrate. The non-crystalline brighter particles are ZnO nanoparticles as indicated by EDX mapping and characteristic chemical composition of ZnO. Zinc acetate readily decomposes to form ZnO nanoparticles at relatively lower temperatures[58-61] and therefore these nanoparticles are likely a result of the unstable nature of zinc acetate solutions. While ZnO formation in solution phase is typically achieved under alkali conditions, it was found that solutions of zinc acetate in DMF without a base left for about an hour or more get cloudy with time. Because of these different species, it is challenging to quantify the crystallite size and surface density on either substrate surface without optimization to achieve only MOF crystallites. I next set out to eliminate zinc oxide nanoparticle formation under our synthesis conditions.
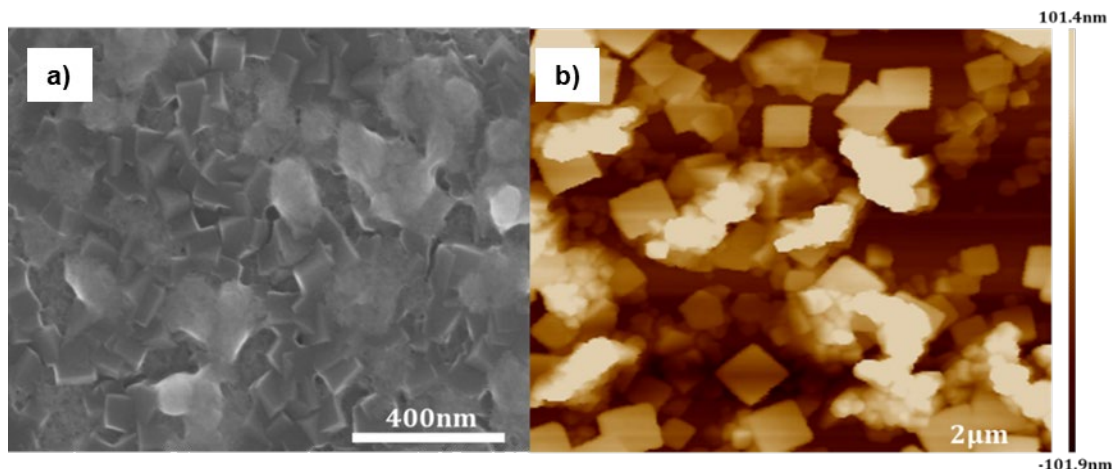
Figure 14: Image of thin films on (a) Silicon wafer, SEM and (b) thermal oxide, AFM (SiO$_2$)

3.2 Effect of metal precursor on thin films growth

Both zinc nitrate and zinc acetate have been used in the synthesis of MOF-5 strutures, specifically using the BDC (benzene dicarboxylic acid) ligand and H$_2$DMCAPZ (dimethyl carboxylic acid pyrazole) ligand. These metal precursors have been used successfully to yield bulk crystals[6, 38-40] and thin films.[41, 42] Both zinc nitrate and zinc acetate have been used to synthesize thin films of zinc-based MOFs such as ZIF-8.[7, 63, 65-67] Thin films of DMCAPZ MOF-5 have been synthesized through dip coating using zinc acetate. Based on this precedent zinc nitrate hexahydrate was initially chosen as the metal precursor for the synthesis of the thin film DMCAPZ MOF-5 using spin-coating method at room temperature *(Figure 15)*.

Using zinc nitrate hexahydrate as the metal precursor for spin coating with solutions of H$_2$DMCAPZ results in no growth of crystalline thin film and instead results in patches of amorphous material *(Figure 15a)*. Changing the metal precursor to zinc acetate instead results in good thin film growth at room temperature *(Figure 15b)*. Due to undesired ZnO nanoparticle growth, a 50/50% by weight ratio of zinc acetate and zinc nitrate was used for synthesis.

34

However, the presence of zinc nitrate inhibits the growth where the growth of cubic crystalline thin films shows consistently smaller crystal sizes *(Figure 15c)*. There is a retention of moderate density of crystals on the surface. For the synthesis of Zn-DMCAPZ MOF increasing the ratio of acetate to nitrate will give thin films with bigger crystal sizes.
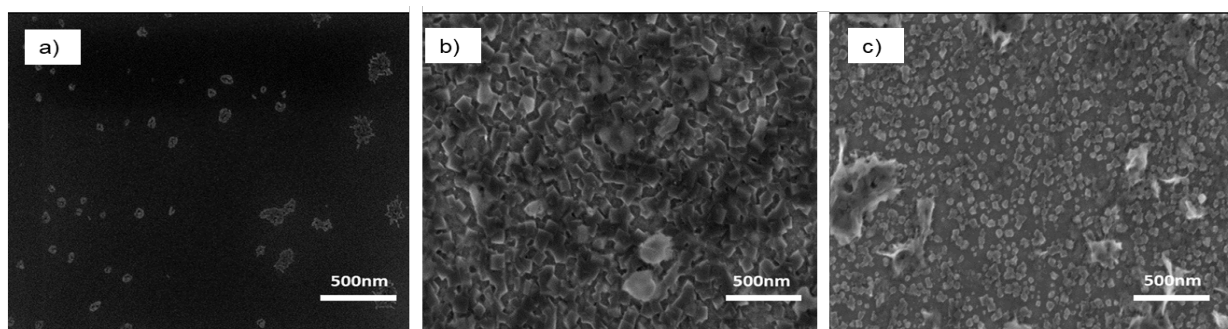
Figure 15: SEM image of thin films for metal precursor study using (a) zinc nitrate (b) zinc acetate (c) 50/50 mix of zinc acetate and zinc nitrate

3.3 Thin film growth on different substrate surfaces

The Zn-based MOF thin film was grown on silicon wafer, thermal oxide (SiO_2) and sapphire (Al_2O_3) using 5 mM zinc acetate solution and 3 mM 3,5-dimethylcarboxylic acid pyrazole (DMCAPZ) solutions in DMF built up layer by layer for 20 cycles. Both surfaces yielded growth of DMCAPZ MOF-5 thin films (Figure 14). There is a higher crystal density of thin film on the thermal oxide and sapphire wafer surfaces (*Figures 16 b-c*) compared to that of silicon wafer *(Figure 16a)*. This is primarily because sapphire and thermal oxide wafers have thicker oxide layers (~300nm) compared to 3 nm of silicon oxide present on silicon wafer. These oxide layers facilitate nucleation and growth. Observing the images in *Figure 16* below, thermal oxide and sapphire also have crystallites of comparable sizes. However, thin films grown on the sapphire surface have slightly higher crystallite sizes and density *(comparing 16c to 16b)*. The insulating property of sapphire (Al_2O_3) and thermal oxides make imaging with SEM difficult due to charging.

Irrespective of these outcomes, silicon wafer was used for optimization due to the ease of imaging using SEM. The other wafer can be used depending on the targeted application.
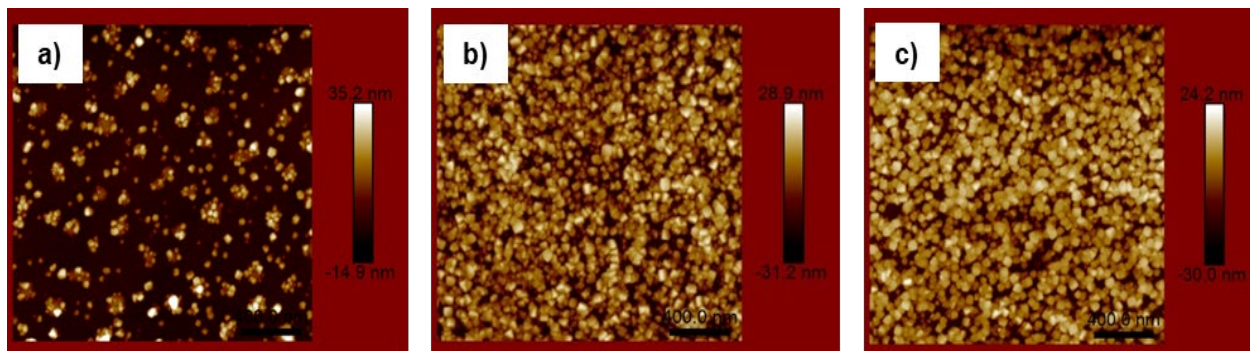
Figure 16: AFM images of thin films substrate study on (a) silicon wafer, (b) thermal oxide and (c) sapphire

3.4 The effect of temperature on thin films growth

In order to determine how temperature affects the growth of DMCAPZ MOF-5 thin films, the precursors were subjected to different temperatures between 25˚C - 50˚C. Results of the thin film growth are shown by SEM in *Figure 17*.

The crystallite size and density of thin films prepared at 25˚C, 30˚C and 40˚C *(Figure 17a- c)* are comparable, therefore the increase in temperature does not significantly affect the crystal distributions or nucleated growth. However, as the temperature increases, the amount and size of zinc oxide nanoparticles increases *(Figure 17)* such that at 50˚C *(Figure 17d)*, there is no observable crystal structure of the MOF. At this temperature large agglomerations and deposition of zinc oxide nanoparticles was observed on the substrate surface. This result is because zinc acetate becomes more unstable as temperature increases and so at temperatures of 50˚C and above, the growth of zinc oxide nanoparticles is thermodynamically and kinetically more favorable than that of DMCAPZ MOF-5 thin film growth. Most of the zinc acetate molecules get converted to

ZnO more readily before they can form zinc oxo-clusters to create nucleation sites for the growth of the MOF crystallites. This result shows that both DMCAPZ MOF-5 crystals and ZnO nanoparticles can be synthesized through the spin-coating method by only altering the temperature of the precursor solutions during synthesis.

There is little difference in size between the thin films made at room temperature, 30˚C and 40˚C and no defined trend exists between them to show that temperature affects the crystal size of the thin film. However, the data shows that the room temperature grown thin film has the largest size of the crystallites. The crystal density data shows that the highest density of the microcrystals sampled at a given nm^2 portion of the substrate surface was observed at 30˚C which is still comparable to room temperature and 40˚C. No observable data was obtained at 50˚C since there was no DMCAPZ MOF-5 thin film growth observed at this temperature. The significant difference between these samples were the increase in zinc oxide growth on the surface as temperature increase from room temperature to 50˚C.
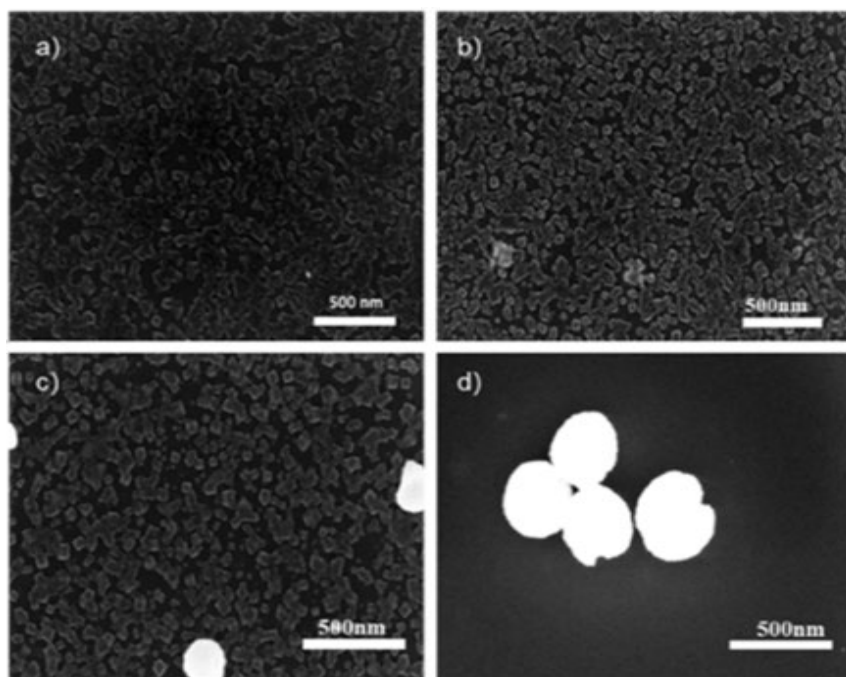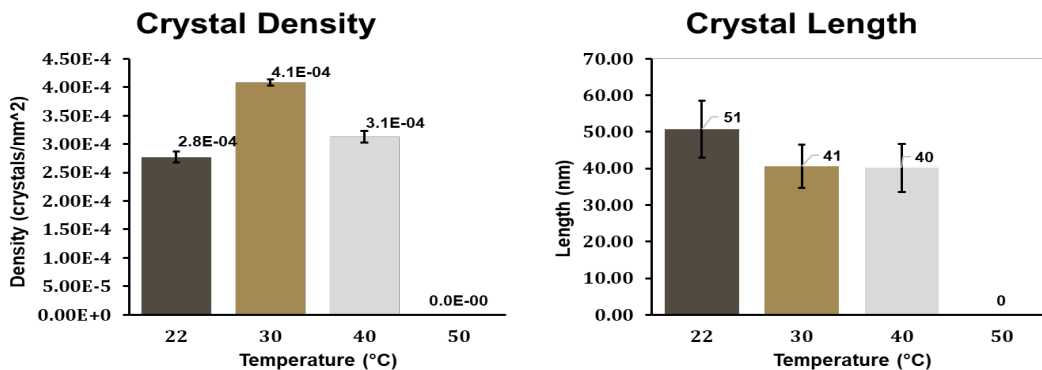
Figure 17: SEM image of the temperature study at (a) room temperature (b) 30°C (c) 40°C and (d) 50°C and crystallite size and density bar graphs

3.5 Effect of solvents on thin films growth

The effect of the solvent is important when considering thin film properties. The solvent is used for making the precursor solutions and as a wash during spin-coating therefore it is necessary to use suitable solvent(s) for the synthesis of thin films. Ethanol and DMF were used as solvents under the same synthesis conditions as they are both prevalent solvents for the Zn-based MOF-5 synthesis.

Ethanol and DMF have been reportedly used to make DMCAPZ MOF-5 both as thin film and bulk crystals.[42] It is important to identify the effect of volatility for the spin-coating process. Thin films made using DMF have well-developed and defined crystal structures with good and uniform coverage *(Figure 18a)*. Thin films synthesized using ethanol as solvent, also show good growth and coverage on the surface, however there is a lack of uniformity in the coverage *(Figure 18b).* Some substrate surface areas show little growth *(upper left-hand corner of Figure 18b)* while aggregated crystallites can be identified at different areas *(right side of Figure 18b)*. This effect ultimately makes surface quantification inconclusive. Additionally, at the very left of *Figure 18* portions of amorphous materials are observed on the surface. When using a 50/50 mixture of

ethanol and DMF, some visible crystallite material with better uniform dispersion of film on the surface is observed, however, the surface is mostly covered by spongy looking amorphous film (*Figure 18c*). The results of this solvent study indicated it best to use DMF as the primary solvent for the synthesis of DMCAPZ MOF-5. Additionally, one of the reasons for the increase in thin films growth may be due to the lower volatility of DMF compared to ethanol. The lower boiling point of DMF may lead to a better moisture environment that can enhance the growth of DMCAPZ MOF-5 compared to ethanol.
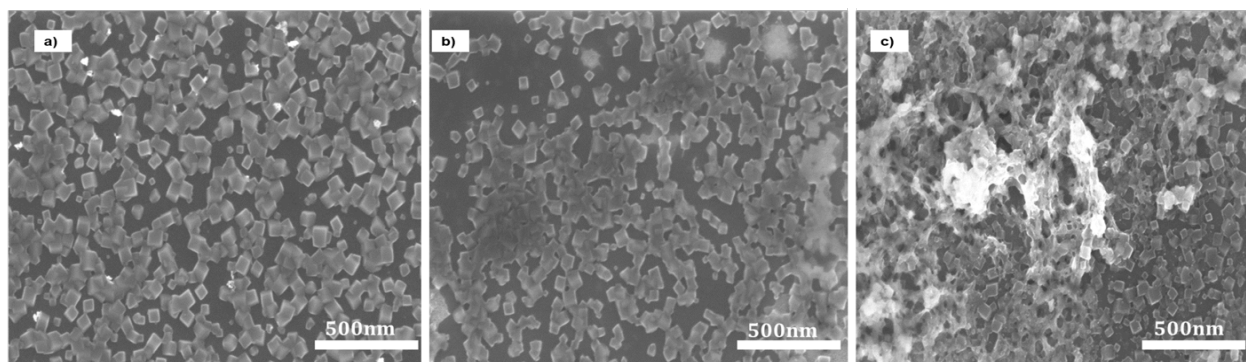
Figure 18: SEM images of thin film solvent study (a) DMF (b) ethanol (c) 50/50 mix of ethanol and DMF

3.6 Optimized DMCAPZ MOF-5 thin film synthesis

Based on the results from the temperature, metal precursor and solvent studies, I developed the optimal conditions for the synthesis of DMCAPZ MOF-5 thin film using a spin-coating method. Combining the best conditions shows DMCAPZ MOF-5 synthesized using zinc acetate dihydrate as metal precursor and DMF as the solvent, at temperature of 25˚C or less and at 25% relative humidity on a bare silicon wafer *(Figure 19)*.

A high density of well-defined and developed microcrystals of DMCAPZ MOF-5 thin film is observed on silicon wafer *(Figure 19a)*. Increasing the magnification allows a closer observation of the defined cubic crystal structure of MOF-5 *(Figure 19b)*. The crystal sizes vary slightly such

that the size of the crystallites is indicative of the nucleation and growth rate of the individual crystals.
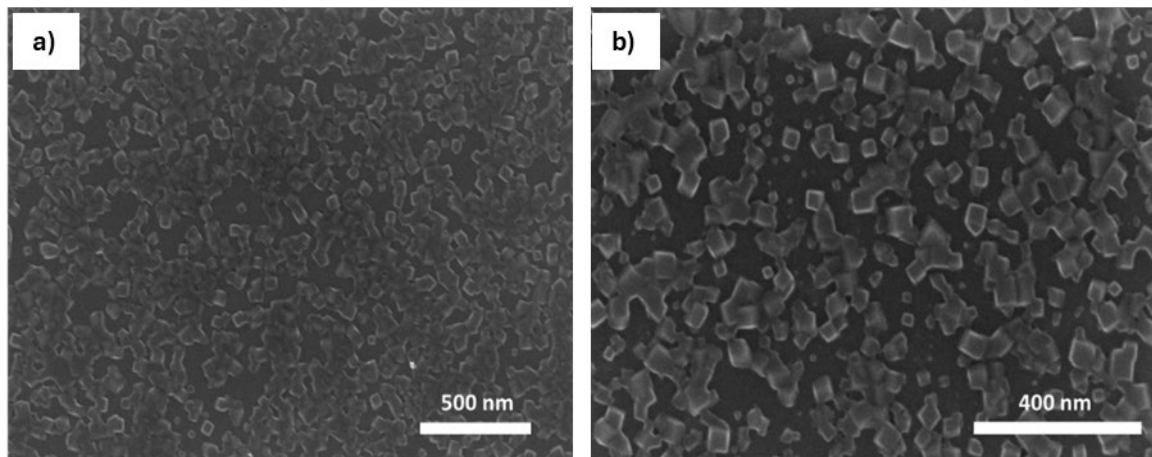
Figure 19: SEM images of optimized thin films made from zinc acetate, using DMF as solvent at (a)80kx and (b) 150kx magnification.

3.7 Piranha treatment of the substrate surface

Increasing the nucleation on the wafer is one way to encourage growth. One of the ways to do this is through treatment with piranha solution which increases the silanol sites on silicon wafer. A piranha solution can be a mix of H_2SO_4/H_2O_2 or HNO_3/H_2O_2. Piranha solutions are typically used for cleaning the top layer of the substrate to remove both dirt from handling and particles from the air. Piranha solution hydroxylates the surface of the silicon wafer through the high oxidizing capability of the hydrogen peroxide. Once the silicon wafer was treated with piranha solution, it was then used as substrate for synthesis of DMCAPZ MOF-5 thin film.

A comparison of the non-pirahna treated substrate for thin film growth and the pirahna treated substrate are shown in Figure 20a-b. These images show that the silicon wafer cleaned with pirahna showed an apparent increase in the crystallite density of the thin film (***Figure 20b compared to Figure 20a)***. Due to some regions of amorphous growth present in the thin film

samples, an additional step was added to make sure the silanols and surface were not too acidic for growth. After treating the wafer with piranha solution, the wafer was next washed with triethylamine, a base that has been employed in the synthesis of MOF powdered crystals.[6] Treatment with base after the piranha wash resulted to a substrate surface with reduced crystal density. However, larger size crystallites with well defined edges appeared to have grown *(Figure 20c)*. The base wash therefore increases the size and crystallinity of individual crystallites, but reduces the crystallite density or amount of nucleation on the surface.
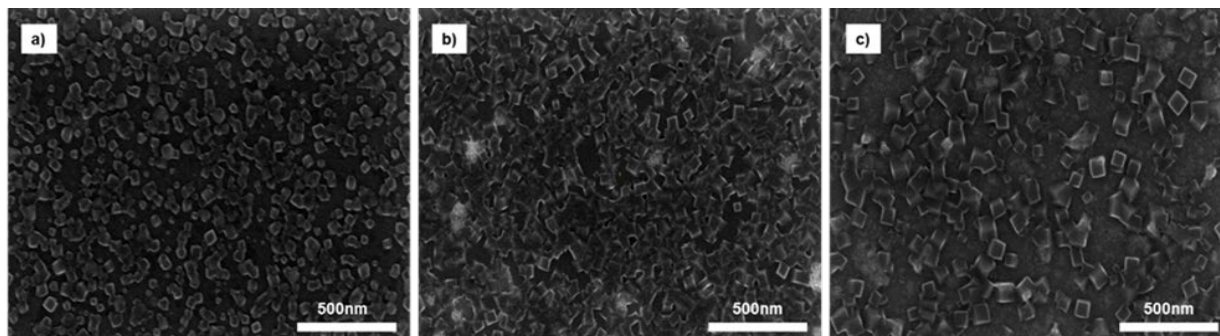
Figure 20: SEM image of thin films wafer treatment study (a) without piranha treatment (b) with piranha (c) washed with base after piranha treatment

3.8 Effect of bimetallic composition on thin films growth

Bimetallic DMCAPZ MOF-5 thin films including copper, cobalt, nickel, aluminum, and zirconium with the zinc were explored because of their useful applications in catalysis and electrochemical activities. Despite the use higher percentage (like 50%) of dopant mentals in other MOF synthetic methods the bimetallics of the Zn-DMCAPZ MOF thin films were not able to BE successfully synthesized at these percentages. Lowering the amount of added metal to 5% provided a path for successfully synthesizing thin Zn-based bimetallic thin films *(Figure 21)*. Aluminum, cobalt, nickel, copper, and zirconium were successfully doped into the DMCAPZ

MOF-5 framework *(Figure 21a-e respectively)*. The crystallinity, shape, size, and density of crystallites varied according the the metal that is added. Aluminum and copper showed the highest level of bright and defined edges of the films *(Figure 21a,d)*. Also, aluminum and zirconium showed the highest level of deformation in the cubic shape of Zn-DMCAPZ MOF. This deformation may be due to the difference in ionic size and charge of zinc (ionic radius = 0.74Å, Zn^{2+}) compared to aluminum (ionic radius = 0.53Å, Al^{3+}) and zirconium (ionic radius = 0.80Å, Zr^{4+})*(Figure 21a,e)*.
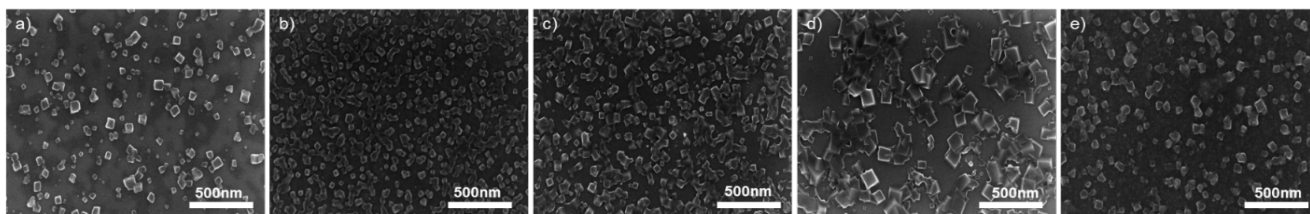
Figure 21: SEM image of bimetallic study, doped with (a) aluminum (b) cobalt (c) nickel (d) copper (e) zirconium

The crystallites were quantified following the process explained in chapter 2 *(Figure 8)*. A graph comparing the crystallite length and density of the different bimetallic DMCAPZMOF-5 thin films shows the differences as a function of metal added (*Figure 22*). Cobalt and nickel doped DMCAPZ MOF-5 has the highest crystallite density while aluminum and zirconium has the least surface densities of the crystallites *(Figure 22b)*. This likely results from the differences in sizes and charges that exist between Zn and those two (Al and Zr). The copper doped MOF thin film has the highest crystallite length while cobalt has the smallest length of crystallites and aluminum, nickel and zirconium bimetallic MOF thin films showed similar lengths of crystallites *(Figure 22a)*. Zirconium has the least amount of crystalinity. This is likely

as result of precursor used which is zirconyl chloride (ZrOCl$_2$) was used for all other bimetallic thin film growth.
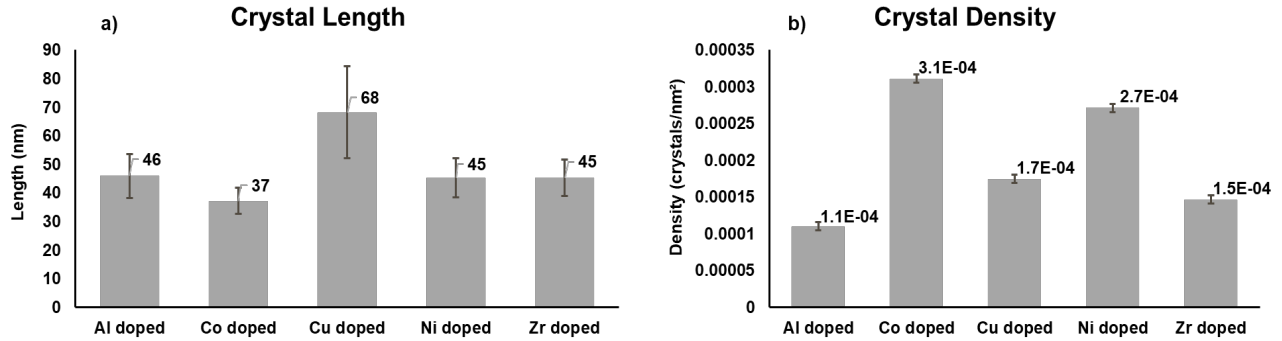
Figure 22: Analysis of the bimetallic thin films with bar graph for (a) crystallite length and (b) crystal density

It was reported that using zirconyl chlorides as a metal precursor resulted in a film with low crystallinity while zirconium chloride [ZrCl$_4$] showed good crystallinity.[51] ZrCl$_4$ was tried as precursor but thin films barely grew. The bimetallic film grown from ZrCl$_4$ showed very sparce growth and small crystallite sizes *(Figure 23).* A similar growth was noticed when cobalt acetate was used in place of cobalt nitrate. This was undesirable, so I opted for zirconyl chloride and the nitrate salts of the dopant metals because even with the low crystallinity of zirconium, all the nitrate salts of the dopant metals and the zirconyl chloride salt gave thin films with better crystallite sizes and density.
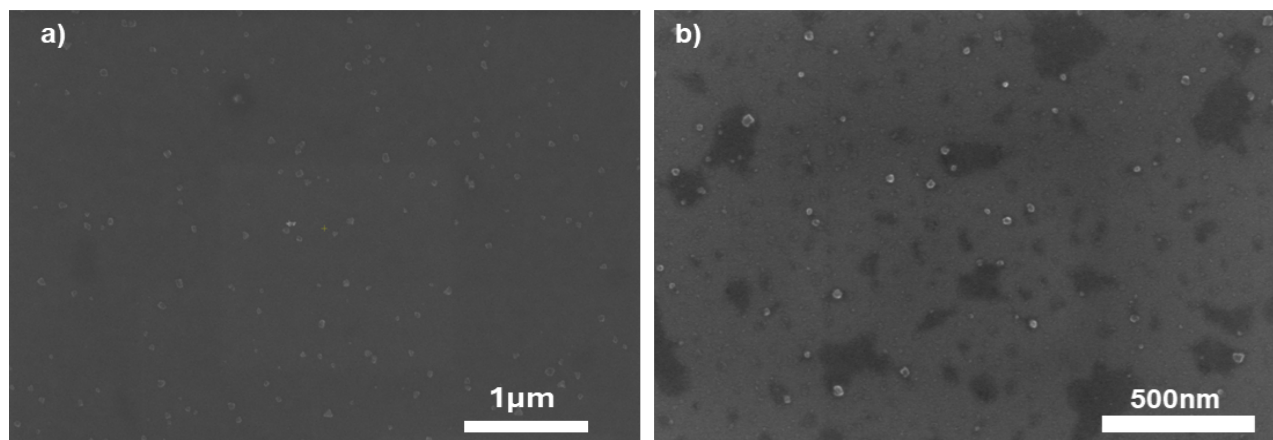
Figure 23: Images showing the Co and Zr bimetallic thin films made with (a) cobalt acetate and (b) zirconium chloride

3.9 Characterization of thin films

3.9.1 Elemental analysis:

To verify the elemental composition of the Zn MOF thin films, XPS was used. This analysis provided the elemental composition of the material and gave information about the chemical environment of the component elements. The composition of the Zn present in the material could be directly related to the presence of silicon which would help us determine the surface coverage present in the material. This is possible because XPS is a surface sensitive technique.

The survey scan of Zn-DMCAPZ MOF thin film is shown in ***Figure 24***. This survey identifies the presence of zinc, carbon, oxygen, and nitrogen which are the components of the MOF structure. The silicon peak in the survey comes from the silicon wafer support. In the ligand structure, there are 6 carbon, 2 nitrogen, and 2 oxygen, so a 3:1:1 ratio of C, N, and O respectively was expected. Based on the structure suggested by Montoro *et al*,[6] the elemental ratio of this material is what the atomic percentage predicts in ***Figure 24***. When you look at the percentage composition of carbon and nitrogen in the survey, it can be seen that C is 32%, 5.5% for N, and 15% for Zn. Oxygen is

44

15%, but that includes those from the substrate surface. From the report derived from the narrow scan of oxygen, only 37% of the oxygen comes from the MOF structure. If you multiply the 15% by 0.3725, (the atomic ratio of carboxylate oxygen species presents on the sample surface) to arrive at 5.6%. This agrees with the amount of nitrogen present since the amount of nitrogen and oxygen in the materials are roughly equal based on the prediction of the structure of the material. The oxygen ratio will exceed the predicted ratio because of the oxygen present on the silicon wafer; there is a small 3-10 nm SiO_2 layer.

The 2s and 2p silicon peaks were easily detected from the survey scan. This indicates that the thin film has pinholes and is not a continuous film over the surface. This is difficult to see in the SEM images, therefore, XPS is useful in clarifying the coverage. The atomic percentages from the survey scan gives an estimate of the amount of silicon wafer surface that is covered by the Zn-DMCAPZ MOF thin film. This shows that about 67.6% of the wafer surface is covered by thin film.
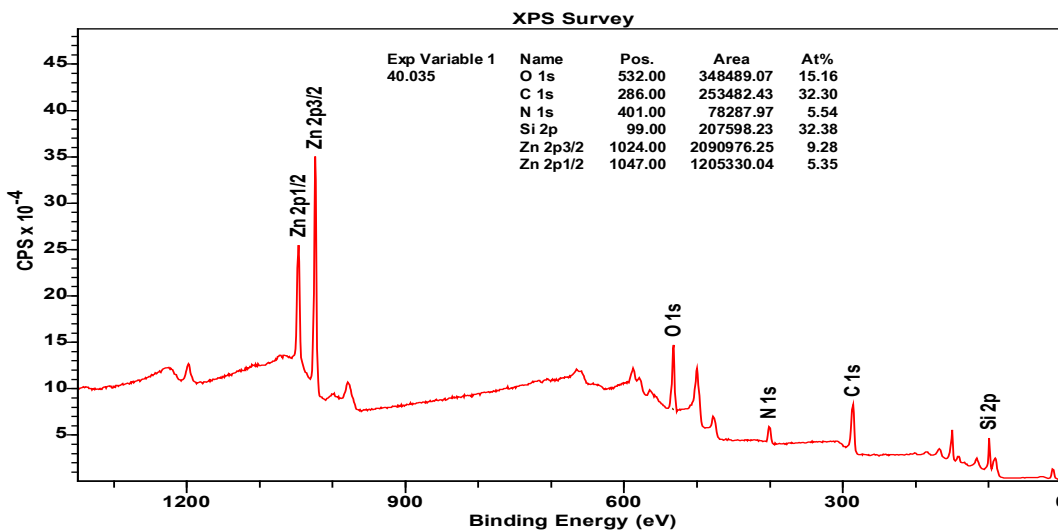
Figure 24: XPS survey scan of the Zn-DMCAPZ MOF thin films.

Furthermore, using the software program CasaXPS analysis of the narrow scans shows the different species of those elements present in the material and oxidation states as well as

chemical environment. The narrow scans of the component elements of Zn-DMCAPZ MOF are shown in *Figure 25*. The two carboxylate oxygens in the ligand are both equivalent and appear in the narrow scan as the minor component at higher binding energy of the oxygen species within the O1s envelope *(Figure 25a)*. However, the oxygen in the SiO_2 (about 3nm) which is less electronegative than carbon, appears at slightly lower binding as the major contributor to the oxygen species. The two nitrogen species present in the $H_2DMCAPZ$ ring are equivalent and thus appear as one peak as seen in the narrow scan of N1s peak which is further confirmed by the symmetric nature of the peak *(Figure 25b)*. Four different carbon species are shown for the C1s narrow scan *(Figure 25c)*. For each $H_2DMCAPZ$ ligand, there are four different carbon atoms, the carboxylate carbon, the equivalent methyl carbons, the equivalent sp^2 carbons that the methyl are connected to and the sp^2 carbon connected to the carboxylate carbon. The red peak which has the highest binding energy belongs to the carboxylate carbon. The taller purple peak is for the two equivalent sp^2 carbons bonded to the methyl groups. The green peak is for the sp^2 carbon that is bonded to the carboxylate carbon while the taller blue peak is for the two equivalents methyl groups. The ratios of these peaks are generally consistent with the ratios of those carbon amounts in the ligand. The narrow scan of Zn 2p (2p3/2 and 2p1/2) shows the 2p peaks which have two symmetric and equal component peaks each for both 2p3/2 and 2p1/2. The peaks at higher binding energies (1024.6 for 2p3/2 and 1047.6 for 2p1/2) represent the zinc species that are surrounded by four oxygen atoms, while the lower binding energies zinc peaks (1023.2 for 2p3/2 and 1046.4 for 2p1/2) belong to the zinc species that are surrounded by 3 nitrogen atoms and 1 oxygen atom (*Figure 25d*). This result shows that there are two zinc species on the material which is consistent with the structure of the framework of Zn-DMCAPZ MOF as shown on *Figure 3b* in chapter 1 of this thesis.
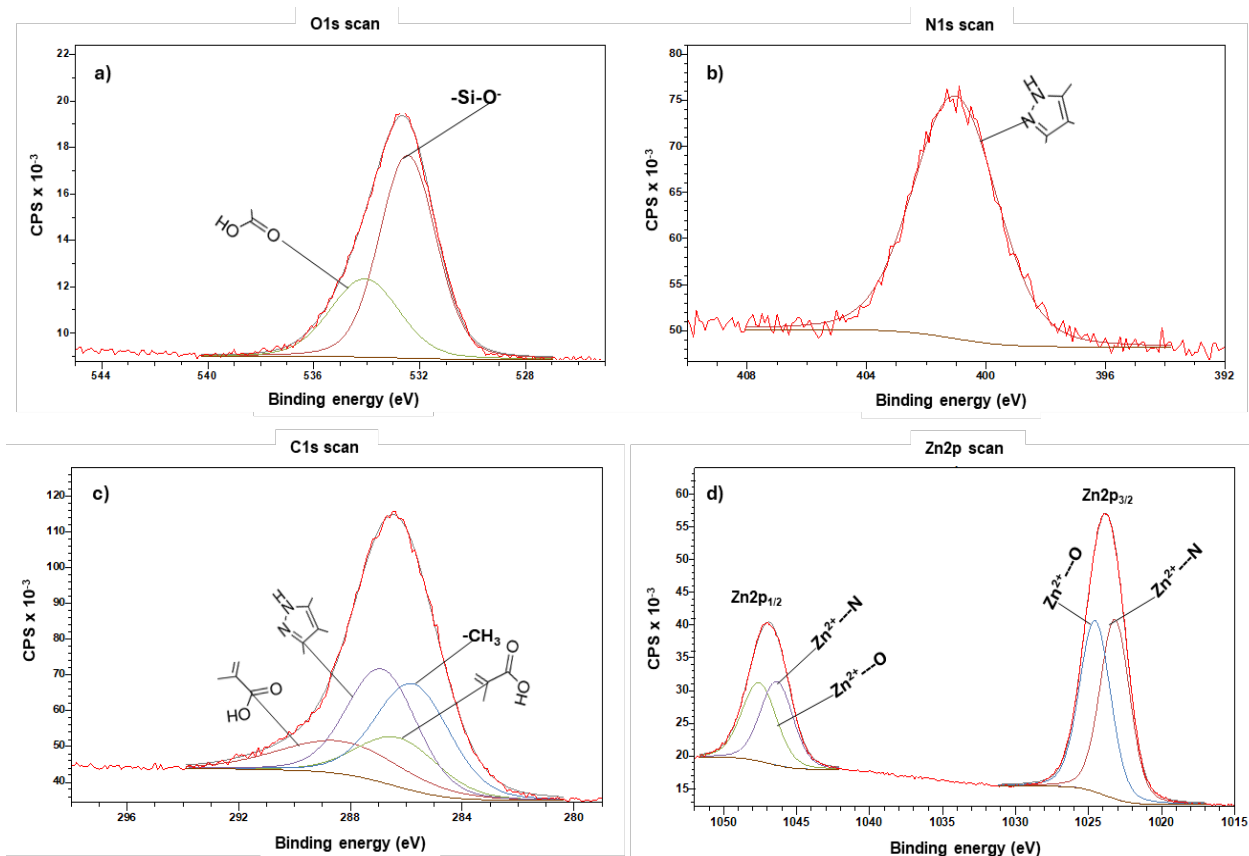
Figure 25: XPS narrow scan of the Zn-DMCAPZ MOF thin films.

The peak positions (in eV) are consistent with all peaks of the metals in their ionic states. The percentage of the dopant metals incorporated affected the peak positions of zinc in both the undoped material, and the bimetallic MOFs is shown in *Table 2.* Zirconium shows the highest amount of incorporation despite the difference between size and charge between Zr^{4+} and Zn^{2+}. This large amount of incorporation can be from Zr having a separate SBU nodal point or sharing a nodal SBU with Zn in the same crystal framework, or separate phases of Zn and Zr crystallite. The peak position of Zn shifts the least (1023.8 to 1023.2 eV for the 2p3/2 peak) with the addition of Zr compared to the other dopant metals. The thin films of the Zr doped MOF have the highest amount of deformation of the cubic structure of the MOF and the least crystallinity of the films *(Figure 19e)*.
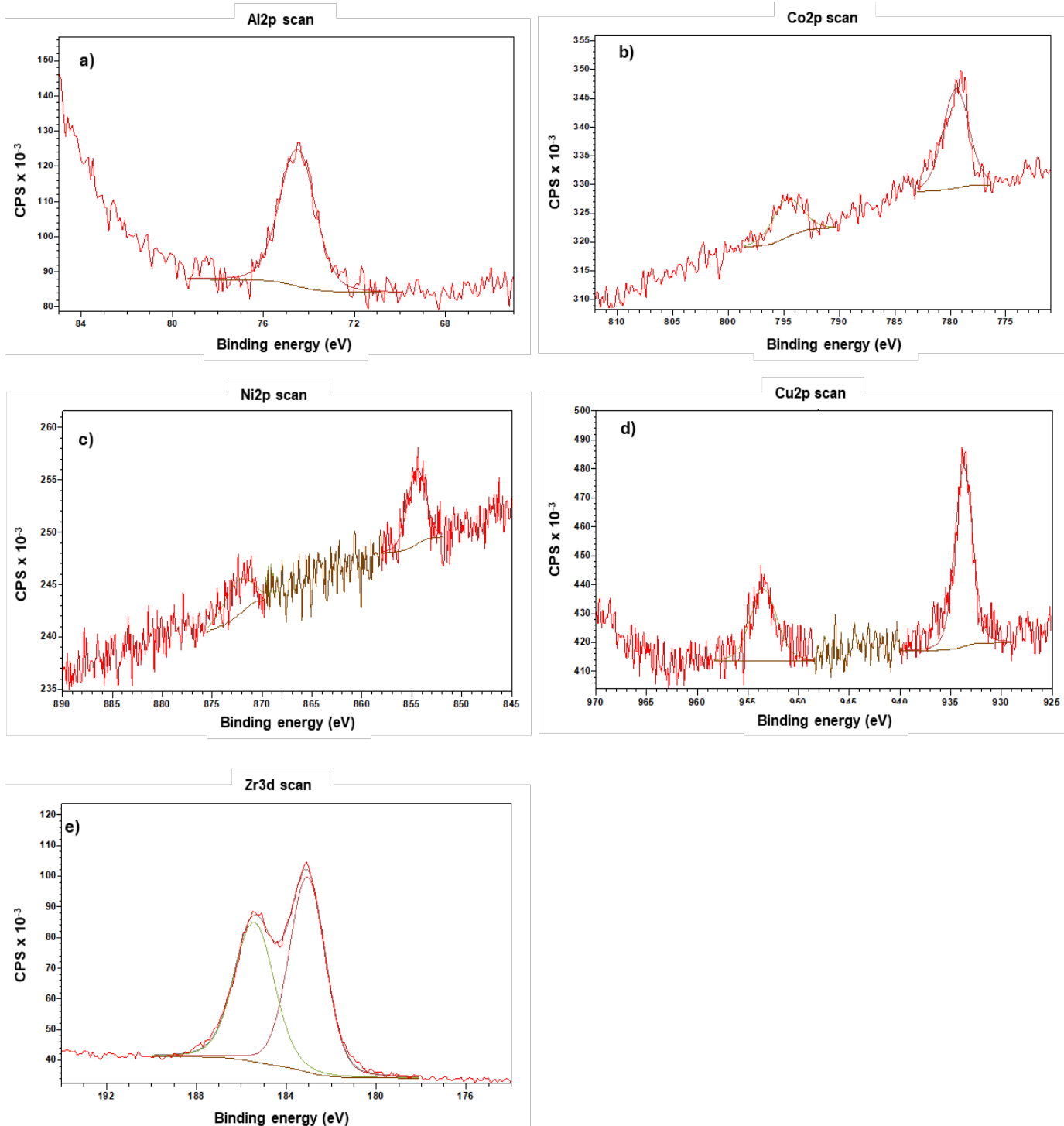
Figure 26: XPS narrow scan of the secondary metals of the bimetallic thin films

Table 2: A table showing the peak positions and composition from XPS

Material type	Zinc peak position (0.0)	Dopant metal peak position (0.0)	Zinc percentage (0.00)	Dopant metal percentage (0.00)
Undoped Zn-DMCAPZ MOF	1023.8 ($2p_{3/2}$) 1046.9 ($2p_{1/2}$)	N/A N/A	100.00 %	0.0 %
Al doped Zn-DMCAPZ MOF	1022.6 ($2p_{3/2}$) 1045.7 ($2p_{1/2}$)	74.5 (2p)	95.09 %	4.91 %
Co doped Zn-DMCAPZ MOF	1022.6 ($2p_{3/2}$) 1045.7 ($2p_{1/2}$)	779.5 ($2p_{3/2}$) 794.8 ($2p_{1/2}$)	97.39 %	2.61 %
Ni doped Zn-DMCAPZ MOF	1023.0 ($2p_{3/2}$) 1046.1 ($2p_{1/2}$)	854.6 ($2p_{3/2}$) 872.4 ($2p_{1/2}$)	99.18 %	0.82 %
Cu doped Zn-DMCAPZ MOF	1022.4 ($2p_{3/2}$) 1045.5 ($2p_{1/2}$)	933.7 ($2p_{3/2}$) 953.4 ($2p_{1/2}$)	96.70 %	3.31 %
Zr doped Zn-DMCAPZ MOF	1023.2 ($2p_{3/2}$) 1046.3 ($2p_{1/2}$)	183.0 ($3d_{5/2}$) 185.4 ($3d_{3/2}$)	86.97 %	13.03 %

3.9.2 X-ray diffraction (XRD analysis)

XRD was used to confirm the crystal structure of the Zn-DMCAPZ MOF thin film by comparing the thin film with reported synthesis of Zn-DMCAPZ MOF both as thin film and as bulk materials. The XRD spectrum below shows the low-angle (a) and mid-angle (b) diffraction pattern of the silicon 111 wafer, the thin film of the Zn-DMCAPZ MOF and the bimetallic thin films (*Figure 27*). Due to the very intense peak of the silicon (111) wafer around 30˚ 2ϴ, the diffraction was cut before and after. Other peaks from the silicon wafer in the XRD data below include the peaks at 9.35˚, 23.3˚, 38.3˚, 59˚, 65.35˚ and 73.8˚ of 2ϴ. The mid angle portion of the XRD spectra of the material is not useful for characterizing the materials. The tall peak at 12.7 2ϴ position for copper might be from a contaminant that was not able to be identify and/or eliminate.

The presence of a (0 2 0) peak at 8.77˚ 2ϴ which is not present in the silicon (111) wafer but is common to the Zn-DMCAPZ MOF thin films can be seen except for the Co doped Zn thin film

(Figure 27b) This peak is typically used to positively identify the structure of the Zn-DMCAPZ MOF, both as thin film and powdered crystals.[6, 42, 55] This characteristic peak is especially important for the thin film, since the possible direction of growth of the thin film crystallites on the substrate is limited compared to a powdered sample, and thus, for thin films, less peaks are observed. The absence of this peak at 8.77° 2ϴ shows that the crystallites of Co-doped Zn thin film did not grow in a direction parallel to the (0 2 0) plane. However, there are other peaks that are not present in the silicon wafer that were present in the Zn-DMCAPZ MOF thin film data that helps confirm that Co-doped Zn-DMCAPZ MOF contains a similar MOF structure. The small peaks at 7.0°2ϴ, 12.45 °2ϴ, and 17.5 °2ϴ are peaks of the MOF crystals and thus a combination of these peaks helps us to determine that all the synthesized bimetallics of Zn-DMCAPZ MOF still retains the MOF structure.

The orientation of the silicon wafer can influence the diffraction pattern in epitaxial crystal growth, so depending on the type of silicon wafer used, different diffraction patterns can be observed. The diffraction pattern of Zn-DMCAPZ MOF where both Si (111) and Si (100) were used to grow Zn-DMCAPZ MOF thin films and its bimetallics is shown in **Figure 28**.
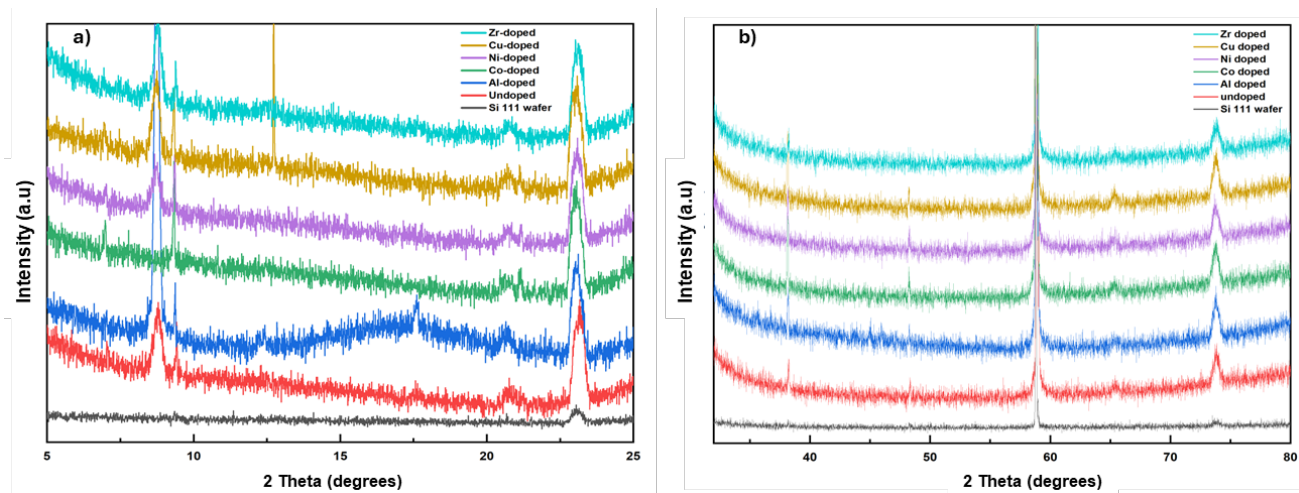
Figure 27: XRD spectra of all thin films on silicon (111) wafer for (a) low angle and (b) mid angle

In *Figure 28*, Co-doped Zn-DMCAPZ MOF showed a small and broad peak at 8.77° but Zr-doped MOF showed no peak at that point. This is the reverse of what is seen in *Figure 27a.* This shows that the most favorable growth orientation for Zn-DMCAPZ MOF is (0 2 0) which is found at 8.77° but that does not mean that all Zn-DMCAPZ MOF based material must have it. The orientation preference might change with synthesis batch and the wafer orientation, but for most cases, the peak at 8.77° is the primary peak most useful for identifying Zn-DMCAPZ MOF crystals, either as thin films or bulk powdered crystals. The orientations of the most prevalent crystallization orientation do not change based on whether there is a (111) or (110) orientation of the silicon wafer. Also, there are multiple peaks coming from the sample and therefore, growth is not presumed to be epitaxial to the surface. Additionally, comparing the growth of the Zn MOF on the Si(111) and Si(110) there is little difference further confirming epitaxial growth is unlikely.

51
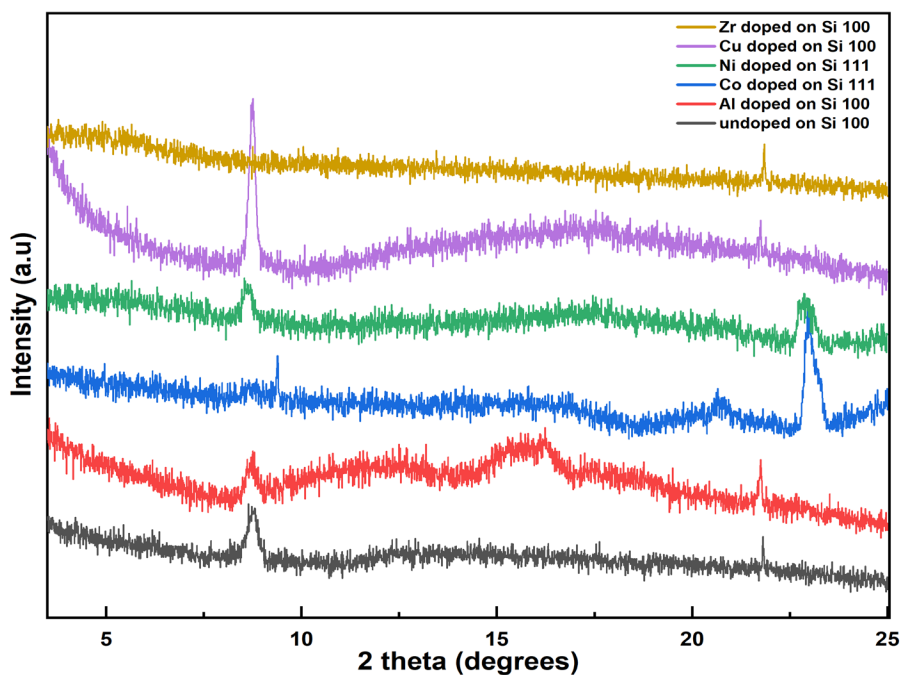
Figure 28: XRD spectra of all thin film on different types of silicon wafers at low angles

CONCLUSION AND FUTURE WORK

4.1 Conclusion

With this work, I have been able to synthesize a Zn-based thin film that has multifunctional application potentials, especially for the capture and conversion of CO_2 to CO which helps to create environmental safety and sustainability while generating a source of energy (CO to fuels). This work showed the optimized synthesis of thin films of Zn-DMCAPZ MOF which are moisture tolerant and nitrogen containing which therefore is capable of binding CO_2 more strongly compared to BDC MOF-5. The synthesis method is cost effective, simple, fast, and completed under ambient conditions.

Some key findings include:

1. Using zinc nitrate resulted in no growth of thin film while zinc acetate gave cubic crystalline thin films of the MOFs but has issue of ZnO nanoparticle formation.

2. Working at low temperature of about 25°C and higher relative humidity of 21% or more helps to reduce zinc oxide nanoparticles. Reducing the concentration of zinc acetate (metal precursor) against the ligand precursor is another strategy to minimize the growth of zinc oxide nanoparticles.

3. Increasing temperature increases the amount of zinc oxide nanoparticles on the sample surface. At 50% and above, no thin film growth is observed, but big ZnO nanoparticles. Higher temperature favors the formation of ZnO.

4. Thin film was successfully grown on silicon, thermal oxide, and sapphire wafers but sapphire had more growth (crystal size and density)

5. For Zn-DMCAPZ MOF, thin film, it was found that DMF works best for the spin coating synthesis process. Ethanol did not work as well as qualitatively. A mix of both solvents (DMF and ethanol) performed the worst.

6. Successfully synthesized and characterized thin film of different bimetallics of Zn-DMCAPZ MOF using a simple, easy, fast, cost-effective and ambient temperature synthesis method.

7. The amount of dopant metal can affect the growth of thin film of material. 5% was found to be the best amount for successful synthesis of the bimetallics thin film of materials.

8. The orientation of crystallites of material appears to be random. The growth of this MOF is non-epitaxial.

9. The difference in ionic size and charge of the dopant metal ion can affect the morphology of the thin film.

10. XPS and XRD were used to characterize the materials synthesized. XPS was used to determine the elemental composition and confirm the structure of the materials peak fitting procedure through the aid of casaXPS peak fitting, quantification, and analysis software. Thus, facts were provided to confirm that the materials of interest were successfully synthesized. I also used XPS to confirm that I was able to successfully incorporate the dopant metals into the Zn-DMCAPZ MOF framework.

11. The crystal structure of the Zn-DMCAPZ MOF was confirmed by comparing the spectra of the individual materials in a single graph and comparing it with data from relevant literature.

Through this research, a standard process and procedure for the wet synthesis of the thin film of Zn-DMCAPZ MOF using the simple, fast, and cost-effective spin coating method has been established. Through this work, I have been able to synthesize high quality thin films of multifunctional zinc-based MOF for variety of applications, specifically, for CO_2 capture and conversion to CO. This material was further improved by making a variety of bimetallic thin films that are expected to perform better in catalysis (electrocatalysis and heterogenous catalysis). Thus, this work has used a simple, cheap, and fast synthesis method, a highly applicable material that can perform multiple functions that would otherwise require multiple expensive materials to perform. This work has created an opportunity for a variety of further studies on the property, further improvement, and application of Zn-DMCAPZ MOF.

4.2 Future work

At the beginning of the research, I started by understanding the material, so as to determine how best to successfully synthesize and make it into a more useful material with diverse application. The research journey involved sharing ideas by a group of smart and talented people with interdisciplinary knowledge, skills and experiences that need to be acquired to achieve success and of those exposure, experiences and contributions helped to make this part of the research work a success. With that being said, the outcome of this work as reported in this thesis is only the beginning of the opportunities that will be explored within the scope of this work. This work has created a foundation for series of possible future work which includes but is not limited to:

1. Further optimization: Study the effect concentrations of precursors on the growth of thin film.
2. Explore further synthesis of bimetallics of other catalytically useful metals.
3. Using the TEM-EDX mapping ability to probe the material to further understand the structure and distribution of the metals (especially the dopant metal) within the bulk of the individual bimetallic material.
4. Devise means to synthesize thin films with very high thickness (more than 5 times the current thickness), so the XRD can be taken full advantage of in order to solve and determine the structure of the bimetallic MOFs and understand what the SBU of the metal center looks like in the different bimetallic MOF thin films so the catalytic activity of the materials can be predicted, which would help inform applications decisions of these materials.

5. Decompose the Zn-DMCAPZ MOF and its bimetallics in the presence of hydrogen to give rise to ZnO nanoparticles and bimetallic nanoparticles that can be applied in heterogeneous catalysis in the ultra-high vacuum chamber to study the catalytic efficiency and mechanism of action of these materials.

6. Explore the best options possible to test activity of the undecomposed MOF and bimetallic MOFs as sorbent material for CO_2 capture and storage, by collaborations.

7. Subsequently, the electrocatalytic activity of these materials can be tested in a simple electrochemical reduction of CO_2 to CO. For this application, both the decomposed and undecomposed Zn-DMCAPZ MOF and their resulting bimetallics can be explored to see how the catalytic activities vary across materials (decomposed vs non-decomposed) and across different bimetallics. This will expose if there are some of the shortcomings that some or all the materials might possess and further study to determine how best to enhance the properties and applications of the materials.

I am excited to see the future of this work and learn more about the capabilities of these materials and the potential to be the next generation of catalyst and sorbent materials amongst other applications.

REFERENCES

(1) Lai, J. Y.; Ngu, L. H.; Hashim, S. S. A review of CO2 adsorbents performance for different carbon capture technology processes conditions. *Greenhouse Gases: Science and Technology* **2021**, *11* (5), 1076-1117.

(2) Qiao, Y.; Wu, C. Nitrogen enriched biochar used as CO2 adsorbents: a brief review. *Carbon Capture Science & Technology* **2022**, *2*, 100018.

(3) Crawford, S. E.; Kim, K.-J.; Yu, Y.; Ohodnicki, P. R. Rapid, selective, ambient growth and optimization of copper benzene-1, 3, 5-tricarboxylate (Cu–BTC) metal–organic framework thin films on a conductive metal oxide. *Crystal Growth & Design* **2018**, *18* (5), 2924-2931.

(4) Varma, R. S.; Baul, A.; Wadhwa, R.; Gulati, S. Introduction to Metal-Organic Frameworks (MOFs). In *Metal-Organic Frameworks (MOFs) as Catalysts*, Springer, **2022**; pp 3-42.

(5) Ibrahim, E.; Cheon, J. N.; Özgür, Y. A. Metal–Organic Framework Materials with Ultrahigh Surface Areas: Is the Sky the Limit? **2012**.

(6) Montoro, C.; Linares, F.; Quartapelle Procopio, E.; Senkovska, I.; Kaskel, S.; Galli, S.; Masciocchi, N.; Barea, E.; Navarro, J. A. Capture of nerve agents and mustard gas analogues by hydrophobic robust MOF-5 type metal–organic frameworks. *Journal of the American Chemical Society* **2011**, *133* (31), 11888-11891.

(7) Zacher, D.; Shekhah, O.; Wöll, C.; Fischer, R. A. Thin films of metal–organic frameworks. *Chemical Society Reviews* **2009**, *38* (5), 1418-1429.

(8) Henke, S. Metal-organic frameworks with additional flexible substituents: modulating responsiveness, gas sorption selectivity & network topologies. Dissertation, Bochum, Ruhr-Universität Bochum, **2011**, 2011.

(9) Dutt, S.; Kumar, A.; Singh, S. Synthesis of metal organic frameworks (MOFs) and their derived materials for energy storage applications. *Clean Technologies* **2023**, *5* (1), 140-166.

(10) Perez, E. V.; Karunaweera, C.; Musselman, I. H.; Balkus Jr, K. J.; Ferraris, J. P. Origins and evolution of inorganic-based and MOF-based mixed-matrix membranes for gas separations. *Processes* **2016**, *4* (3), 32.

(11) Janiak, C.; Vieth, J. K. MOFs, MILs and more: concepts, properties and applications for porous coordination networks (PCNs). *New Journal of Chemistry* **2010**, *34* (11), 2366-2388.

(12) Raptopoulou, C. P. Metal-organic frameworks: Synthetic methods and potential applications. *Materials* **2021**, *14* (2), 310.

(13) Stock, N.; Biswas, S. Synthesis of metal-organic frameworks (MOFs): routes to various MOF topologies, morphologies, and composites. *Chemical reviews* **2012**, *112* (2), 933-969.

(14) Khan, M. S.; Shahid, M. Synthesis of metal-organic frameworks (MOFs): routes to various MOF topologies, morphologies, and composites. In *Electrochemical Applications of Metal-Organic Frameworks*, Elsevier, **2022**; pp 17-35.

(15) San Ho, P.; Chong, K. C.; Lai, S. O.; Lee, S. S.; Lau, W. J.; Lu, S.-Y.; Ooi, B. S. Synthesis of Cu-BTC metal-organic framework for CO2 capture via solvent-free method: effect of metal precursor and molar ratio. *Aerosol and Air Quality Research* **2022**, *22* (12), 220235.

(16) Pachfule, P.; Das, R.; Poddar, P.; Banerjee, R. Solvothermal synthesis, structure, and properties of metal organic framework isomers derived from a partially fluorinated link. *Crystal Growth & Design* **2011**, *11* (4), 1215-1222.

(17) Fu, Z.; Xu, G. Crystalline, highly oriented MOF thin film: The fabrication and application. *The Chemical Record* **2017**, *17* (5), 518-534.

(18) Shi, X.; Shan, Y.; Du, M.; Pang, H. Synthesis and application of metal-organic framework films. *Coordination Chemistry Reviews* **2021**, *444*, 214060.

(19) Sabzehmeidani, M. M.; Kazemzad, M. Recent advances in surface-mounted metal–organic framework thin film coatings for biomaterials and medical applications: a review. *Biomaterials Research* **2023**, *27* (1), 115.

(20) Shekhah, O. Layer-by-layer method for the synthesis and growth of surface mounted metal-organic frameworks (SURMOFs). *Materials* **2010**, *3* (2), 1302-1315.

(21) Chen, D.-H.; Gliemann, H.; Wöll, C. Layer-by-layer assembly of metal-organic framework thin films: Fabrication and advanced applications. *Chemical Physics Reviews* **2023**, *4* (1).

(22) Ahn, H.; Kim, S.; Xu, R.; Lee, J. W.; Kang, Y. T. Structural modified metal-organic frameworks by hierarchical layer-by-layer method for efficient CO2 capture enhancement. *Journal of CO2 Utilization* **2023**, *77*, 102603.

(23) Hinman, J. G.; Turner, J. G.; Hofmann, D. M.; Murphy, C. J. Layer-by-layer synthesis of conformal metal–organic framework shells on gold nanorods. *Chemistry of Materials* **2018**, *30* (20), 7255-7261.

(24) Ma, Z.-Z.; Li, Q.-H.; Wang, Z.; Gu, Z.-G.; Zhang, J. Electrically regulating nonlinear optical limiting of metal-organic framework film. *Nature Communications* **2022**, *13* (1), 6347.

(25) Chernikova, V.; Shekhah, O.; Eddaoudi, M. Advanced fabrication method for the preparation of MOF thin films: Liquid-phase epitaxy approach meets spin coating method. *ACS applied materials & interfaces* **2016**, *8* (31), 20459-20464.

(26) Rocío-Bautista, P.; Taima-Mancera, I.; Pasán, J.; Pino, V. Metal-organic frameworks in green analytical chemistry. *Separations* **2019**, *6* (3), 33.

(27) Do, H. H.; Truong, H. B. Ni, Co, Zn, and Cu metal-organic framework-based nanomaterials for electrochemical reduction of CO2: A review. *Beilstein Journal of Nanotechnology* **2023**, *14* (1), 904-911.

(28) Adkins, H.; Cramer, H. I. The use of nickel as a catalyst for hydrogenation. *Journal of the American Chemical Society* **1930**, *52* (11), 4349-4358.

(29) Gupta, S.; Fernandes, R.; Patel, R.; Spreitzer, M.; Patel, N. A Review of Cobalt-Based Catalysts for Sustainable Energy and Environmental Applications. *Applied Catalysis A: General* **2023**, 119254.

(30) Dey, S.; Dhal, G. The catalytic activity of cobalt nanoparticles for low-temperature oxidation of carbon monoxide. *Materials Today Chemistry* **2019**, *14*, 100198.

(31) Ben David, R.; Ben Yaacov, A.; Head, A. R.; Eren, B. Methanol decomposition on copper surfaces under ambient conditions: mechanism, surface kinetics, and structure sensitivity. *ACS catalysis* **2022**, *12* (13), 7709-7718.

(32) Stoddart, A. Perfecting copper catalysts. *Nature Synthesis* **2023**, 1-1.

(33) Han, S.; Ciufo, R. A.; Wygant, B. R.; Keitz, B. K.; Mullins, C. B. Methanol oxidation catalyzed by copper nanoclusters incorporated in vacuum-deposited HKUST-1 thin films. *ACS Catalysis* **2020**, *10* (9), 4997-5007.

(34) Cao, H.; Liu, S.; Wang, X. Environmentally benign metal catalyst for the ring-opening copolymerization of epoxide and CO2: state-of-the-art, opportunities, and challenges. *Green Chemical Engineering* **2022**, *3* (2), 111-124.

(35) Ni, C.; Ma, X.; Yang, Z.; Roesky, H. W. Recent advances in aluminum compounds for catalysis. *European Journal of Inorganic Chemistry* **2022**, *2022* (10), e202100929.

(36) Peng, L.; Zhao, Y.; Yang, T.; Tong, Z.; Tang, Z.; Orita, A.; Qiu, R. Zirconium-Based Catalysts in Organic Synthesis. *Topics in Current Chemistry* **2022**, *380* (5), 41.

(37) Chen, S.; Tennakoon, A.; You, K.-E.; Paterson, A. L.; Yappert, R.; Alayoglu, S.; Fang, L.; Wu, X.; Zhao, T. Y.; Lapak, M. P. Ultrasmall amorphous zirconia nanoparticles catalyse polyolefin hydrogenolysis. *Nature Catalysis* **2023**, *6* (2), 161-173.

(38) Hajiashrafi, S.; Kazemi, N. M. Preparation and evaluation of ZnO nanoparticles by thermal decomposition of MOF-5. *Heliyon* **2019**, *5* (9).

(39) Li, J.; Cheng, S.; Zhao, Q.; Long, P.; Dong, J. Synthesis and hydrogen-storage behavior of metal–organic framework MOF-5. *international journal of hydrogen energy* **2009**, *34* (3), 1377-1382.

(40) Saha, D.; Wei, Z.; Deng, S. Hydrogen adsorption equilibrium and kinetics in metal–organic framework (MOF-5) synthesized with DEF approach. *Separation and Purification Technology* **2009**, *64* (3), 280-287.

(41) Hou, C.; Peng, J.; Xu, Q.; Ji, Z.; Hu, X. Elaborate fabrication of MOF-5 thin films on a glassy carbon electrode (GCE) for photoelectrochemical sensors. *RSC advances* **2012**, *2* (33), 12696-12698.

(42) Bétard, A.; Wannapaiboon, S.; Fischer, R. A. Assessing the adsorption selectivity of linker functionalized, moisture-stable metal–organic framework thin films by means of an environment-controlled quartz crystal microbalance. *Chemical Communications* **2012**, *48* (85), 10493-10495.

(43) Du, S.; Yang, J.; Qu, S.; Lan, Z.; Sun, T.; Dong, Y.; Shang, Z.; Liu, D.; Yang, Y.; Yan, L. Impact of precursor concentration on perovskite crystallization for efficient wide-bandgap solar cells. *Materials* **2022**, *15* (9), 3185.

(44) Zhong, M.; Kong, L.; Zhao, K.; Zhang, Y. H.; Li, N.; Bu, X. H. Recent progress of nanoscale metal-organic frameworks in synthesis and battery applications. *Advanced Science* **2021**, *8* (4), 2001980.

(45) Xu, X.; Yang, J.; Hong, Y.; Wang, J. Nitrate precursor driven high performance Ni/Co-MOF nanosheets for supercapacitors. *ACS Applied Nano Materials* **2022**, *5* (6), 8382-8392.

(46) Das, A.; Vemuri, R.; Kutnyakov, I.; McGrail, B.; Motkuri, R. An efficient synthesis strategy for metal-organic frameworks: dry-gel synthesis of MOF-74 framework with high yield and improved performance, Sci. Rep. **2016** 6, 1–7.

(47) Zhang, D.; Zhang, X.; Bu, Y.; Zhang, J.; Zhang, R. Copper cobalt sulfide structures derived from MOF precursors with enhanced electrochemical glucose sensing properties. *Nanomaterials* **2022**, *12* (9), 1394.

(48) Lu, X.; Liu, Y.; He, Y.; Kuhn, A. N.; Shih, P.-C.; Sun, C.-J.; Wen, X.; Shi, C.; Yang, H. Cobalt-Based Nonprecious Metal Catalysts Derived from Metal–Organic Frameworks for High-Rate Hydrogenation of Carbon Dioxide. *ACS applied materials & interfaces* **2019**, *11* (31), 27717-27726.

(49) Sargazi, G.; Afzali, D.; Ghafainazari, A.; Saravani, H. Rapid synthesis of cobalt metal organic framework. *Journal of Inorganic and Organometallic Polymers and Materials* **2014**, *24*, 786-790.

(50) Chin, J. M.; Chen, E. Y.; Menon, A. G.; Tan, H. Y.; Hor, A. T. S.; Schreyer, M. K.; Xu, J. Tuning the aspect ratio of NH 2-MIL-53 (Al) microneedles and nanorods via coordination modulation. *CrystEngComm* **2013**, *15* (4), 654-657.

(51) Ardila-Suárez, C.; Rodríguez-Pereira, J.; Baldovino-Medrano, V. G.; Ramírez-Caballero, G. E. An analysis of the effect of zirconium precursors of MOF-808 on its thermal stability, and structural and surface properties. *CrystEngComm* **2019**, *21* (9), 1407-1415.

(52) Chen, W.-C.; Chen, S.; Yu, T.-Y.; Su, J.; Chen, H.-P.; Lin, Y.-W.; Cheng, C.-P. Growth of Si3N4 Thin Films on Si (111) Surface by RF-N2 Plasma Nitriding. *Coatings* **2020**, *11* (1), 2.

(53) Zhang, J.; Cheng, H.; Chen, Y.; Uddin, A.; Yuan, S.; Geng, S.; Zhang, S. Growth of AlN films on Si (100) and Si (111) substrates by reactive magnetron sputtering. *Surface and Coatings Technology* **2005**, *198* (1-3), 68-73.

(54) Ellis, J. E.; Crawford, S. E.; Kim, K.-J. Metal–organic framework thin films as versatile chemical sensing materials. *Materials Advances* **2021**, *2* (19), 6169-6196.

(55) Wannapaiboon, S.; Tu, M.; Fischer, R. A. Liquid Phase Heteroepitaxial Growth of Moisture-Tolerant MOF-5 Isotype Thin Films and Assessment of the Sorption Properties by Quartz Crystal Microbalance. *Advanced Functional Materials* **2014**, *24* (18), 2696-2705.

(56) Semrau, A. L.; Zhou, Z.; Mukherjee, S.; Tu, M.; Li, W.; Fischer, R. A. Surface-mounted metal–organic frameworks: Past, present, and future perspectives. *Langmuir* **2021**, *37* (23), 6847-6863.

(57) Anderson, H. C.; Rawlins, M.; Prue, A. A.; Sanders, L. M.; Rivera, F.; Stowers, K. J. Tunable CuO nanostructured thin films derived from metal–organic frameworks for dehydrogenation of alcohols. *Journal of Materials Chemistry A* **2022**, *10* (34), 17680-17690.

(58) Kołodziejczak-Radzimska, A.; Jesionowski, T. Zinc oxide—from synthesis to application: a review, Materials **2014** 7 2833–2881.

(59) Mahato, T.; Prasad, G.; Singh, B.; Acharya, J.; Srivastava, A.; Vijayaraghavan, R. Nanocrystalline zinc oxide for the decontamination of sarin. *Journal of hazardous materials* **2009**, *165* (1-3), 928-932.

(60) Duan, Y.; Li, J.; Yang, X.; Hu, L.; Wang, Z.; Liu, Y.; Wang, C. Kinetic analysis on the non-isothermal dehydration by integral master-plots method and TG–FTIR study of zinc acetate dihydrate. *Journal of Analytical and Applied Pyrolysis* **2008**, *83* (1), 1-6.

(61) Ghule, A. V.; Ghule, K.; Chen, C. Y.; Chen, W. Y.; Tzing, S. H.; Chang, H.; Ling, Y. C. In situ thermo-TOF-SIMS study of thermal decomposition of zinc acetate dihydrate. *Journal of Mass Spectrometry* **2004**, *39* (10), 1202-1208.

(62) Ibach, H.; Carette, J.; Feuerbacher, B. *Electron spectroscopy for surface analysis*; Springer, **1977**.

(63) Chaudhari, A.; Souza, B.; Tana, J. Electrochromic thin films of Zn-based MOF-74 nanocrystals facilely grown on flexible conducting substrates at room temperature featured. APL Mater. **2019**, 7, 081101, 2019.

(64) Rousso, I.; Deshpande, A. Applications of atomic force microscopy in HIV-1 research. *Viruses* **2022**, *14* (3), 648.

(65) Luu, C. L.; Nguyen, T.; Nguyen, A. P.; Hoang, C. T.; Ha, A. C. Multifunctional Zn-MOF-74 as the gas adsorbent and photocatalyst. *Advances in Natural Sciences: Nanoscience and Nanotechnology* **2020**, *11* (3), 035008.

(66) Panella, B.; Hirscher, M.; Pütter, H.; Müller, U. Hydrogen adsorption in metal–organic frameworks: Cu-MOFs and Zn-MOFs compared. *Advanced Functional Materials* **2006**, *16* (4), 520-524.

(67) Falcaro, P.; Ricco, R.; Doherty, C. M.; Liang, K.; Hill, A. J.; Styles, M. J. MOF positioning technology and device fabrication. *Chemical Society Reviews* **2014**, *43* (16), 5513-5560.